Received: 19 May 2023 | Revised: 22 July 2024 | Accepted: 29 July 2024

DOI: 10.1002/esp.5957

RESEARCH ARTICLE

ESPL WILEY

A mathematical model for bedrock incision in near-threshold gravel-bed rivers

Vanessa Gabel[1,2] | Gregory E. Tucker[1,2] | Benjamin Campforts[3,4]

[1]Cooperative Institute for Research in Environmental Sciences (CIRES), University of Colorado Boulder, Boulder, Colorado, USA

[2]Department of Geological Sciences, University of Colorado Boulder, Boulder, Colorado, USA

[3]Department of Earth Sciences, VU University Amsterdam, Amsterdam, The Netherlands

[4]Institute for Arctic and Alpine Research (INSTAAR), University of Colorado Boulder, Boulder, Colorado, USA

Correspondence
Vanessa Gabel, Cooperative Institute for Research in Environmental Sciences (CIRES), University of Colorado Boulder, Boulder, CO, USA.
Email: vanessa.gabel@colorado.edu

Funding information
National Aeronautics and Space Administration, Grant/Award Number: 80NSSC22K0465; Directorate for Geosciences, Grant/Award Numbers: 1822062, 2100702, 2104102, 2148762

Abstract

Gravel-bed rivers that incise into bedrock are common worldwide. These systems have many similarities with other alluvial channels: they transport large amounts of sediment and adjust their forms in response to discharge and sediment supply. At the same time, the occurrence of bedrock incision implies behaviour that falls on a spectrum between fully detachment-limited 'bedrock channels' and fully transport-limited 'alluvial channels'. Here, we present a mathematical model of river profile evolution that integrates bedrock erosion, gravel transport and the formation of channels whose hydraulic geometry is consistent with that of near-threshold alluvial channels. We combine theory for five interrelated processes: bedload sediment transport in equilibrium gravel-bed channels, channel width adjustment to flow and sediment characteristics, abrasion of bedrock by mobile sediment, plucking of bedrock and progressive loss of gravel-sized sediment due to grain attrition. This model contributes to a growing class of models that seek to capture the dynamics of both bedrock incision and alluvial sediment transport. We demonstrate the model's ability to reproduce expected fluvial features such as inverse power law scaling between slope and area, and width and depth consistent with near-threshold channel theory, and we discuss the role of sediment characteristics in influencing the mode of channel behaviour, erosional mechanism, channel steepness and profile concavity.

KEYWORDS
alluvial river, bedrock river, gravel-bed river, river profile evolution, sediment abrasion

1 | INTRODUCTION

Rivers on Earth showcase an enormous diversity of morphologies, flow regimes and erosional and depositional behaviours. However, current mathematical models for river profile evolution usually address only a restricted range of behaviour and often conflate morphology and behaviour. For example, mathematical models are often formulated to address cases with either 'bedrock' channel morphology or 'alluvial' channel morphology (Howard & Kerby, 1983; Tucker & Whipple, 2002; Whipple & Tucker, 1999; Willgoose et al., 1991a). Bedrock channels are typically associated with upland landscapes undergoing active erosion, meaning that these channels incise bedrock. Their behaviour is often considered detachment-limited (Howard, 1994), meaning that their rate of erosion is limited by the river's ability to detach bedrock from the riverbed; their widths are confined by bedrock, which limits their lateral mobility, and sediment is often assumed to be exported rapidly from these systems, such that its long-term effects on channel evolution may be either neglected or parameterized in terms of a time-averaged bulk sediment flux (e.g.,Whipple & Tucker, 2002). Alluvial channels are associated with lowland settings and are assumed to primarily transport sediment, which leads their profile evolution to be 'transport-limited'. These channels commonly have mobile banks, leading to greater lateral mobility, and many have been found to adjust their width to exert just the shear stress on their beds necessary to move a median grain size; these are termed 'equilibrium channels' or 'near-threshold channels' (Phillips et al.2022).

Gravel-bed rivers may be best described as a subset of alluvial rivers, but some also exhibit behaviours of 'bedrock' rivers, such as active incision into bedrock that may be partially exposed in otherwise

alluvial bed and banks. Naming conventions appear to be unsettled: what are likely gravel-bed rivers, at least through some reaches, have been referred to in the literature as 'sediment-load dominated bedrock channels' (Johnson et al., 2009), 'gravel-rich bedrock channels' (Lai et al., 2021) and 'quasi-alluvial channels' (Pitlick & Cress, 2002), amongst other terms. These channels occur in montane erosional settings, and therefore, we can reasonably assume that they incise bedrock over sufficiently long timescales. Yet these channels also adhere to many of the tenets of alluvial river behaviour. For example, their forms may be linked to basin-scale supply conditions (Pfeiffer et al., 2017) or in-channel sediment characteristics (Parker, 1978; Phillips & Jerolmack, 2016): the latter case is termed a 'threshold' or 'near-threshold' river, wherein channel geometry is closely adjusted to exert just the shear stress on the riverbed required to transport the median grain size under bankfull flow conditions, while maintaining stable banks. This is commonly represented as:

$$\tau_b^* = (1+\epsilon)\tau_c^* \quad (1)$$

where ϵ is an empirically derived factor with a value ≈ 0.2 (Parker, 1978), τ_c^* is the critical Shields stress, and τ_b^* is the dimensionless Shields stress on the riverbed at bankfull flow conditions. Derivations of the terms and form that constitute (1) can be found in Shields (1936) and Parker (1978), and the substantial degree of scatter to be found in measurements of τ_b^* has been documented and discussed by Buffington and Montgomery (1997). For the purpose of this manuscript, however, we simply observe that self-formed gravel-bed channels tend to have $\tau_b^* \approx 0.03 - 0.07$ (Buffington & Montgomery, 1997). Not only do gravel-bed rivers have a somewhat predictable shear stress regime, but their forms also cluster with other alluvial rivers around near-threshold predictions for hydraulic geometry (Phillips et al., 2022). Analysis of these types of channels has also revealed that sediment supply and transport set the channel slope and consume a significant portion of the river's energy budget (Johnson et al., 2009; Lai et al., 2021), and they can be modelled using transport-limited formulations (Wickert & Schildgen, 2019). Taken together, these observations point to a discrepancy between what is often observed in field settings (river beds mantled with alluvium and mobile channel banks) and our large-scale understanding of geologic systems (that rivers set in mountain ranges are working to lower those ranges).

The prevalence of gravel-bed rivers worldwide suggests the need for mathematical models to represent river systems that incise rock over long time scales while also maintaining alluvial-like morphology most of the time and transporting substantial quantities of coarse sediment. We currently lack an understanding of how broadly applicable the idea of a near-threshold channel might be; however, some bedrock-incising rivers do show evidence of near-threshold behaviour, implying that this type of geomorphic adjustment does apply to at least a subset of bedrock-incising channels. A few examples of rivers with bankfull shear stress similar to a threshold channel prediction include the Colorado River (Colorado and Utah, USA; $\tau_b^* \approx 0.05$), the Agness River (Oregon, USA; $\tau_b^* \approx 0.065$), and the Rio Mameyes (Puerto Rico; $\tau_b^* \approx 0.06$) (Phillips et al., 2022). These example rivers all drain rugged and/or rocky terrain in mountainous regions, including places with active seismicity. While there are clear examples of rivers that should not conform to near-threshold channel predictions (e.g., when banks are composed of bedrock rather than self-formed from gravel in active transport, or when valley confinement is such that overbank flows produce shear stresses far in excess of the bankfull shear stress), we nevertheless can identify channels that appear to incise bedrock while also being described by near-threshold behaviour. This observation opens an interesting question: What are the implications for long-term channel profile evolution if we allow for near-threshold behaviour in a bedrock-incising fluvial model? It is also interesting to consider where this theory is not capable of reproducing observed morphology to identify its current range, applicability and future improvements.

Finally, there is an additional process, common to coarse-bedded alluvial and bedrock rivers alike, that has been mostly neglected in models of longitudinal profile evolution and landscape evolution to date: the progressive downstream loss of gravel bedload to attrition (Attal & Lavé, 2006). Field studies have shown that the attrition of gravel-size sediment can be substantial in mountain river systems (Dingle et al.2017), yet we have only a rudimentary understanding of how such loss might influence patterns and rates of landscape evolution.

This study has two primary aims: articulating a simple mathematical model for river profile development, which includes bedrock erosion, gravel transport, grain attrition and near-threshold channel adjustment, and determining the extent to which that model captures basic properties of incising river networks. To these ends, we first outline the model's governing equations based on prevailing theory and current models of bedrock incision and sediment transport. Combining these equations, we then seek an analytical solution to a simplified form of the model. Finally, we nondimensionalize our analytical solution in order to reveal the fundamental parameter groups that govern model response. Identifying nondimensional parameter groups reduces the number of free parameters in the model, allowing us to proceed with a more constrained sensitivity analysis of model behaviour. We focus the analysis on steady rather than transient profiles, with an examination of the model's ability to reproduce widely observed steady state fluvial forms, such as an inverse slope-area relationship. Here, our aim is only to present and analyse the mathematical formulation as it applies in a steady, one-dimensional case; scaling the model up to two dimensions would be appropriate for a follow-up study.

2 | BACKGROUND

The stream power incision model (Howard & Kerby, 1983; Seidl & Dietrich, 1992; Whipple & Tucker, 1999) has achieved widespread use in modelling the evolution of river profiles and fluvially sculpted topography. It is appealing for both its intuitive, physically based nature, and for its ability to reproduce certain characteristics of river profiles, such as transient, upstream-migrating knickpoints and concave-up steady state profiles (Lague, 2014). However, the stream power model's inability to capture sediment dynamics within the river system makes it less applicable to bedrock-incising gravel-bed rivers. The recognition that sediment indeed plays an important role in bedrock river evolution has led to the development of a number of mechanistic abrasion models, also called sediment-flux-dependent incision models, that account for sediment effects.

Many researchers have argued that sediment flux should provide a strong control on bedrock incision rates either through providing tools to abrade the bed, cover to protect the bed, or both (Beaumont et al., 1992; Foley, 1980; Gilbert, 1877; Sklar & Dietrich, 1998). Sklar and Dietrich (2001) performed experiments to demonstrate and quantify how saltating bedload sediment is capable of incising bedrock via abrasion, a process that involves bedrock being gradually chipped away as a result of particle impacts. The authors recognized that the effect is nonlinear: at low sediment supply rates, the sediment grains act as abrasive tools that promote erosion of the bed; as supply increases, increasing sediment cover on the bed inhibits further erosion. Whipple and Tucker (2002) provided a simple mathematical framework for these effects that combines elements of the stream power incision model with a sediment-flux-dependent incision rate; later work by Sklar and Dietrich (2004) resulted in mechanistic model that treats erosion as a function of the kinetic energy of particle impacts on bedrock. Gasparini et al. (2006) further explored the nonlinearity of sediment-driven erosion by testing channel response in cases where increasing sediment flux only inhibits erosion, as compared with cases in which erosion can be either enhanced or inhibited by increased sediment supply. Their model also incorporates a stream power-dependent erosion rate, but differs from Whipple and Tucker (2002) by allowing for some erosion to occur even at negligible supply rates, which presumably reflects plucking or other erosional processes (Gasparini et al., 2006). Chatanantavet and Parker (2009) developed a model in which both plucking and abrasion by bedload contribute to lowering bed elevation; importantly, they also included a 'macroabrasion' process to capture the idea that abrasion not only removes bedrock through particle impacts, but also plays a role in weakening bedrock via fracturing and thereby priming bedrock to be plucked. Zhang et al. (2015) developed an abrasion model built upon work by Sklar and Dietrich (2001,2004), but they handled bedrock cover by comparing the total thickness of alluvium on the riverbed to a macro-roughness height. This allows their model to simulate progressive bedrock exposure, leading to a gradual, rather than instantaneous, response to changes in supply conditions.

The development of abrasion models has allowed for exploration of how sediment influences the bedrock incision process. However, sediment dynamics can also give rise to spatial transitions between more detachment-limited and more transport-limited behaviour (Gasparini et al., 2006; Whipple & Tucker, 2002). This phenomenon has been explored through the development of mathematical models that capture both the removal of material from the riverbed and the re-deposition of that material downstream; we refer to these as 'erosion-deposition models'. One such model, proposed by Beaumont et al. (1992), calculates sediment transport capacity as a function of slope and water discharge and relates the rate of erosion to the deficit between capacity and actual sediment supply, analogous to a first-order chemical reaction rate. Deposition occurrs where supply exceeds local capacity. A model by Davy and Lague (2009) extends this concept by introducing a sediment transport length scale that depends on discharge and an effective settling velocity parameter (see also Hergarten, 2020b). If this transport distance is short relative to the system of interest, their model is effectively transport-limited, while a long transport distance results in detachment-limited behaviour. Shobe et al. (2017) advanced this concept further by incorporating a dynamic sediment layer on top of bedrock. Their formulation allows for a time- and space-varying bedrock exposure fraction, which in turn modulates rates of sediment entrainment and bedrock erosion. Turowski and Hodge (2017) took a different approach to variable bedrock exposure by creating a probabilistic model for sediment deposition on a partially alluviated bed, explicitly accounting for the areal extent of sediment cover. Similar to Davy and Lague (2009) and Shobe et al. (2017), this model allows for gradual, rather than instantaneous, reductions in bed cover and increases in transport rate.

Advances in both mechanistic abrasion models and erosion-deposition models have improved our understanding of the role of sediment in the evolution of both bedrock rivers and mixed bedrock-alluvial rivers. However, most of these models rely on an imposed empirical relationship between width and discharge (e.g., Chatanantavet & Parker, 2009; Gasparini et al., 2006; Shobe et al., 2017). An important limitation of such empiricism is that it fails to account for the tendency of gravel-bed rivers to adjust their bankfull width and depth to local flow and sediment conditions (Parker, 1978). The inability to accommodate channel width dynamics also limits the extent to which bedrock and alluvial processes can create meaningful feedbacks, for example, channel widening, which could result from grain size reduction due to grain attrition (the process of clasts reducing in size downstream as a result of repeated impacts with other clasts and the riverbed), should result in more bedrock becoming exposed to erosion by plucking and abrasion. However, this feedback cannot be captured if channel width is simply imposed as a boundary condition. This example also highlights another shortcoming: relatively few models account for streamwise modification of the sediment load due to grain attrition and selective transport, both of which are well-documented processes that alter the character of sediment in a river (e.g., Attal & Lavé, 2006, 2009; Dingle et al., 2017; Menting et al., 2015; Parker, 1991; Sklar et al.2006).

3 | METHODS

Here, we present a 1D profile evolution model for bedrock-incising, gravel-bedded rivers (Figure 1). Our model draws on theory and observation that support the following assumptions: (1) plucking and abrasion are the most significant processes in bedrock erosion, (2) bedrock becomes exposed gradually, rather than exposure being treated as an 'on/off' switch, (3) gravel-bed rivers adhere to near-threshold alluvial geometries, and (4) sediment is modified streamwise via attrition. At any point along the profile, channel bed elevation is the sum of bedrock elevation plus some thickness of sediment that mantles the riverbed. We borrow from Wickert and Schildgen (2019) in maintaining constant bankfull bed shear stress and near-threshold alluvial geometry in the modelled channel and in the conception of mass conservation within a fixed-width valley, rather than a fixed-width channel. At equilibrium, the bedrock erosion rate is equivalent to the imposed rock uplift rate relative to baselevel, and the thickness of the alluvial layer is constant through time. The model is designed to represent channels that have at least one bank composed of potentially mobile alluvial sediment, such that the channel width and depth would readjust quickly to any changes in bankfull discharge or slope; therefore, the model does not address bedrock-confined channels or the mechanics of lateral bedrock erosion. Additionally, because we assume valleys have fixed width, a close accounting of the factors that

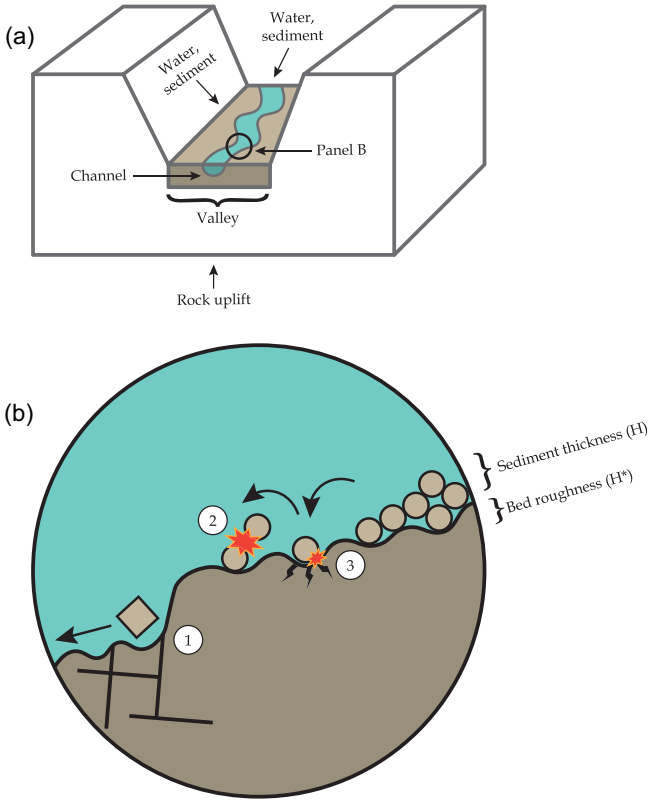

FIGURE 1 Schematic illustration of model behaviour. In panel (a), a channel of variable width is set into a valley of fixed width. Sediment is delivered to the channel from upstream and from the surrounding basin. Panel (b) shows the model's in-channel processes: bedrock is eroded through plucking (1) and abrasion by sediment in transport (3). Sediment attrition occurs as a function of sediment flux (2). Impacts that cause sediment attrition and bedrock abrasion are represented by red and yellow starbursts. Sediment thickness (H) on the riverbed can be spatially variable, and the amount of sediment required to fully cover the bed depends on bed roughness (H^*). [Color figure can be viewed at wileyonlinelibrary.com]

set valley width (e.g.,Langston & Temme, 2019; Tofelde et al., 2022) is beyond the scope of this paper.

In brief, the model erodes bedrock and sediment from the channel bottom, carries a fraction of that eroded material as bedload in the channel and loses some fraction of bedload mass downstream to grain attrition. We assume that rock erosion occurs only through plucking and abrasion, as these are assumed to be the dominant erosional processes in bedrock rivers (Whipple, 2004). The efficiency of bedrock erosional processes is modulated by the fraction of exposed bedrock in the riverbed at each point along the profile. Like Shobe et al. (2017), we treat the bedrock exposure fraction as a continuouos variable rather than a binary 'on/off switch'. Finally, rather than treating gravel-size sediment as wholly indestructible, we mimic the observation that coarse sediment loses mass downstream due to particle attrition (Attal & Lavé, 2006; Dingle et al., 2017; Sklar & Dietrich, 2001; Sklar et al., 2006). Importantly, however, this model assumes a constant grain size for gravel: rather than tracking size reduction of individual grains, we model gravel attrition by tracking and updating the total volume of bedload sediment in transport. Effectively, then, there are two size fractions: a gravel-size fraction that is tracked as bed load, and a fraction consisting of fine sediment, derived partly from abrasion, that is evacuated from the system as wash load without deposition.

Together, these concepts provide the basis for a model that hypothesizes that gravel-bed rivers may incise bedrock while also appearing and behaving like alluvial channels. In the sections below, we first outline the governing equations and then describe the methodology for testing the model.

3.1 | Governing equations

The fundamental equation in our model that determines how river profiles evolve through time states that the rate of change of total elevation is equal to the rate of change of bedrock elevation, plus the rate of change of some thickness of sediment that sits atop the bedrock profile:

$$\frac{\partial \eta}{\partial t} = \frac{\partial \eta_b}{\partial t} + \frac{\partial H}{\partial t} \tag{2}$$

where η is the total topographic elevation [L], η_b is the bedrock elevation [L], and H is the sediment thickness [L]. Note that H represents only the coarse fraction of sediment that travels as bed load; we assume that finer suspended and wash load material is efficiently removed from the system and composes only a negligible fraction of deposited sediment at any given time. Each term on the right hand side can be broken down into its contributing pieces: bedrock elevation is controlled by uplift of rock relative to baselevel (hereafter 'uplift rate') and by bedrock erosion, and sediment thickness depends on the generation of coarse material from bedrock plucking, lateral input from the surrounding basin, the along stream sediment flux, and the loss of coarse sediment volume due to grain attrition. The general forms of these equations are as follows:

$$\frac{\partial \eta_b}{\partial t} = \text{uplift rate} - \text{erosion rate} \tag{3}$$

$$\frac{\partial H}{\partial t} = \text{coarse sediment generation} + \text{lateral sediment supply} + \text{sediment influx} - \text{sediment outflux} - \text{grain attrition} \tag{4}$$

Erosion and sedimentation rates in our model depend upon an interaction between bed exposure, sediment flux, bedrock pluckability and sediment hardness. These interactions are outlined in equations below.

3.2 | Varying-width channel within a fixed-width valley

Mass is conserved within a valley of fixed width, while a channel with varying hydraulic radius exerts control on local sediment transport and erosion rates. To represent valley width, B, we use the approach of Wickert and Schildgen (2019), which treats valley width as a power function of streamwise distance, x, downstream of the channel head:

$$B = k_{xB} x^{P_{xB}} \tag{5}$$

where $P_{x,B}$ is a dimensionless valley width exponent with a value >0 and $k_{x,B}$ is a valley width coefficient with a value >1 and dimensions of $[L^{1-P_{x,B}}]$.

We assume that channels obey the near-threshold principle, by which bankfull channel width adjusts to provide stable banks and mobile bed sediment under bankfull flow conditions. This form of near-equilibrium behaviour has been demonstrated for many natural gravel-bed channels and arises from the tendency of channels with erodible banks to widen until the stresses applied to the banks fall below the threshold for entrainment and transport (Parker, 1978; Parker et al., 2007; Phillips & Jerolmack, 2016, 2019). Wickert and Schildgen (2019) showed that near-threshold theory implies that bankfull channel width should depend on bankfull discharge, Q [L^3/T], slope gradient, S, and median grain diameter, D_{50} [L]:

$$b = k_b \frac{QS^{7/6}}{D_{50}^{3/2}} \tag{6}$$

The coefficient k_b lumps together factors for gravitational acceleration, sediment density, water density and the dimensionless Shields stress. Wickert and Schildgen (2019) estimated its value as $k_b \approx 2.61$ $s/m^{3/2}$, or 8.3×10^{-8} $year/m^{3/2}$.

We represent discharge as the product of drainage basin area, A, [L^2] and r, the bankfull runoff rate [L/T]:

$$Q = rA \tag{7}$$

A simple form of Hack's law (Montgomery & Dietrich, 1992) is used to relate drainage area to streamwise position:

$$A = \frac{1}{3}x^2 \tag{8}$$

See Wickert and Schildgen (2019) for full derivations of B and b.

3.3 | Bed exposure

We define the fractional area of the bed over which bedrock is exposed under bankfull conditions as α. While several studies have explored controls on sediment cover and bedrock exposure (e.g., Chatanantavet & Parker, 2008; Finnegan et al., 2007; Goode & Wohl, 2010; Hodge et al., 2011; Hodge & Hoey, 2016; Inoue et al., 2016; Johnson et al., 2009; Johnson & Whipple, 2010; Johnson, 2014), the quantitative nature of the relationship between sediment cover and bedrock exposure remains unsettled. Previous workers have hypothesized an exponential relationship, either between bed exposure and the ratio of transport to capacity (Turowski et al., 2007), or directly between bed exposure and sediment thickness (Shobe et al., 2017). This type of exponential model has been shown in laboratory-scale experiments to be well-suited to channels with rough beds (Mishra & Inoue, 2020). Here, we follow Shobe et al. (2017) in hypothesizing an exponential relationship relating sediment thickness to bedrock exposure:

$$\alpha = e^{-H/H^*} \tag{9}$$

Here, H represents the spatially averaged sediment thickness present on the riverbed [L], and H^* is a characteristic height that is presumed to scale with the roughness height [L] of the bedrock underlying the alluvial layer. When the sediment thickness is large relative to the roughness height, bed exposure is minimized; when sediment cover is thin relative to the roughness scale, bed exposure is maximized. This factor modulates the effectiveness of bedrock erosion and sediment transport processes (Figure 2).

The precise manner of the scaling relationship between sediment cover thickness (H) and bedrock exposure (α) remains an open question that would benefit from careful field study. The physical meaning of H^* is also somewhat ambiguous and could likewise be clarified by detailed field measurements: for example, does this quantity represent a range of bedrock roughness values, or a standard deviation? Here, we treat H^* as a generic scaling factor whose value is important only insofar as it controls the amount of sediment required to fully cover the bed. We favour the exponential formulation not only for its numerical simplicity and ability to smoothly transition from fully exposed to fully covered bed conditions, but also because it represents a testable hypothesis: bed exposure fraction (α), average sediment thickness (H) and bedrock roughness height (H^*) could all be measured in the field to refine the relationship between these three quantities and to clarify their physical meanings.

3.4 | Sediment flux

The bedload transport function derives from the relation of Meyer-Peter and Müller (1948), as modified by Wong and Parker (2006), in which transport rate depends on excess Shields stress (where Shields stress is the bed shear stress normalized by the weight of a one-grain-thick layer of sediment). Near-threshold channel adjustment leads to a situation in which the bankfull Shields stress, τ^*, tends to maintain a constant value slightly higher (by a factor $\epsilon \approx 0.2$ Parker, 1978; Phillips & Jerolmack, 2019) than the threshold for

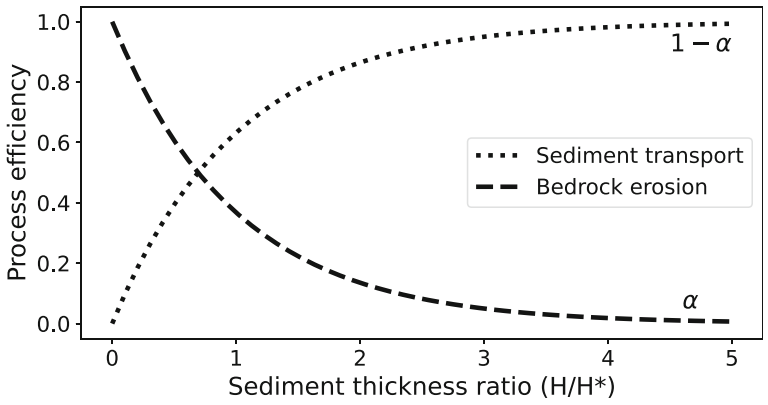

FIGURE 2 The ratio of sediment thickness to characteristic roughness height controls the efficiency of sediment transport and bedrock erosion processes. The bedrock erosion line is equivalent to α, the bedrock exposure fraction, and the sediment transport line is $1-\alpha$. Equations related to bedrock erosion are multiplied by α, and sediment transport calculations are multiplied by $1-\alpha$.

entrainment of the median-size channel sediment, τ_c^*. An interesting outcome of this near-equilibrium state is a roughly constant bankfull rate of bedload transport per unit channel width, because bankfull excess Shields stress is approximately uniform in the streamwise direction (e.g., Pitlick & Cress, 2002). Thus, for near-threshold channels, variations in bankfull bed-load transport rate arise mainly from variations in channel width, which itself depends on discharge and slope, via Equation (6) above. Wickert and Schildgen (2019) combined the Meyer–Peter and Müller bedload transport formula with Equation (6) to yield an expression for total volumetric bedload transport rate ($[L^3/T]$) under bankfull flow. Their derivation results in a sediment flux function that depends on slope, discharge and flow intermittency; here, we modify their expression by incorporating a bed cover factor that expresses the inhibition of sediment transport when only a fraction of the bed is covered by sediment:

$$Q_s = k_{Qs} I Q S^{7/6} (1-\alpha) \tag{10}$$

Here, k_{Qs} is a lumped, dimensionless coefficient whose value assumes a constant shear stress slightly above that needed to transport the median grain size at bankfull conditions (Parker, 1978) and I is an intermittency factor that describes how often geomorphically effective flows occur within the channel. Wickert and Schildgen (2019) estimated a value of 0.041 for k_{Qs} and used $I = 0.01$ as a representative intermittency factor for bankfull flow. The factor $(1-\alpha)$ describes the fraction of the riverbed covered by sediment. When α is sufficiently small, the bed is effectively 100% covered by mobile sediment and sediment flux, Q_s, will be maximized.

3.5 | Bedrock erosion

We assume that bedrock erosion may occur through two mechanisms: plucking and abrasion by bedload. In general, the effectiveness of both mechanisms should depend on the fraction of bedrock exposed on the riverbed. A computational analysis by Hurst et al. (2021) highlighted the role of dynamic pressure differences in plucking fracture-bounded blocks. Whipple et al. (2000) proposed that the time-averaged rate of erosion by plucking should scale with pressure fluctuations, which would in turn scale with excess fluid shear stress. In the spirit of these analyses, we start from the premise that the rate of bedrock lowering by plucking in a channel at bankfull flow, E_{bf}, depends on excess Shields stress multiplied by an efficiency factor, p, and by the fractional bedrock exposure α,

$$E_{bf} = p(\tau_b^* - \tau_c^*)\alpha. \tag{11}$$

In a near-threshold channel with approximately constant bankfull Shields stress, this becomes

$$E_{bf} = p\epsilon\tau_c^* \alpha. \tag{12}$$

where ϵ represents the fraction by which bankfull shear stress on the riverbed exceeds the above the threshold for grain entrainment (Parker, 1978; Phillips & Jerolmack, 2019).

The above expression represents the instantaneous rate of bedrock lowering in the active channel under bankfull flow. To convert it to a time-averaged rate of rock lowering per unit valley floor area, it is necessary to multiply Equation (12) by the intermittency factor I and by the channel-to-valley width ratio b/B, to obtain

$$E_p = Ibp\epsilon\tau_c^* \alpha/B \tag{13}$$

Substituting (6) for b, we arrive at a discharge-slope formulation for the plucking rate:

$$E_p = \frac{k_b p\epsilon\tau_c^*}{D_{50}^{3/2}} I Q S^{7/6} \alpha/B \tag{14}$$

It is convenient to lump the various prefactors into a single efficiency coefficient, K, to arrive at a simple plucking rate function:

$$E_p = KI\frac{Q}{B}S^{7/6}\alpha \tag{15}$$

Apart from the slight nonlinearity on the slope factor, this erosion rate expression has the general form of stream power per unit valley floor area. It is consistent with the results of Dubinski and Wohl (2013), who found a linear relationship between stream power and plucking rate in bedrock. K has traditionally been referred to as the bedrock 'erodibility'; here, we will refer to K as the 'pluckability' factor, in order to distinguish its role in the plucking component of bedrock erosion, rather than abrasion. K has dimensions $[1/L]$. As in (10), I represents a fraction of time during which geomorphically effective flows occur.

Abrasion is accomplished through sediment impacts on the riverbed. We adopt the abrasion formulation of Chatanantavet and Parker (2009), in which the volume rate of material removal by sediment impacts per unit channel length depends on the abrasion coefficient of the bedrock substrate, ζ ($[1/L]$), and the volumetric bed-load sediment flux. As before, we also incorporate the fraction of bedrock exposed:

$$E_a = \zeta\frac{Q_s}{B}\alpha \tag{16}$$

While both E_p and E_a include factors related to rock strength, the pluckability factor used in (15) depends more on large-scale bedrock features such as jointing, while the abrasion coefficient used in (16) is related to strength at the grain scale. In practice, plucking likely dominates where bedrock is extensively fractured, while abrasion may dominate in more massive rock or rock with relatively low tensile strength. We assume that while both of these erosion processes contribute to lowering bedrock elevation, only plucking contributes to the gravel flux; all erosion generated via abrasion is treated as fines and is thus not tracked in our model. The total bedrock erosion rate ($[L/T]$) is simply the sum of plucking and abrasion:

$$E_b = E_p + E_a \tag{17}$$

3.6 | Attrition

In addition to sediment abrading the riverbed, gravel clasts in transport also undergo grain size reduction through impacts with both the riverbed and other clasts; this is one of the principal mechanisms at

play in downstream fining (e.g., Attal & Lavé, 2009; Kodama, 1994). We refer to this grain-on-grain action as 'attrition' in order to differentiate it from bedrock abrasion; here the term abrasion will refer solely to vertical lowering of the elevation profile resulting from grain impacts on bedrock exposed in the riverbed. The volume rate of grain attrition per unit valley length, ψ [L^2/T], is a function of the attrition coefficient of the sediment comprising the bedload, β [1/L] and gravel transport rate:

$$\psi = \beta Q_s \tag{18}$$

The attrition coefficient represents the fraction of sediment that is lost per unit length of transport; correspondingly, $1/\beta$ is the e-folding length for downstream volume loss to attrition. This value is most often determined experimentally (e.g., Attal & Lavé, 2006), but may also be deduced from field studies that examine changes in grain size by lithology along stream or that measure compressive pebble strength using a Schmidt hammer (e.g., Pfeiffer et al., 2022).

The default model behaviour is to treat the abrasion coefficient of sediment, β, as being equal to the abrasion coefficient of bedrock, ζ, which represents bedrock and sediment composed of the same material. However, these parameters need not be the same and may be expected to differ when an upstream sediment source dominates the sediment load (see Section 4). Note that for simplicity, we treat attrition as a process that reduces the volume flux but not the median diameter of bed-load sediment.

3.7 | Lateral sediment supply

Sediment is eroded from the surrounding drainage basin at a rate controlled by bedrock erosion in the main channel and enters the valley through a network of tributaries. As in the main channel, any sediment moving through the tributary system will be subject to attrition; therefore, the lateral sediment flux to the valley at any point will be a function of the distance travelled. In the absence of grain attrition ($\beta = 0$), the lateral sediment supply increases linearly with the length of the incoming tributary channel; when grain attrition is accounted for ($\beta > 0$), lateral sediment supply becomes a saturating exponential function with tributary length. This relationship is expressed as such

$$q_L = \begin{cases} \dfrac{E_b \gamma x}{3} & \text{if } \beta = 0 \\ \dfrac{E_b \gamma}{\beta}\left(1 - e^{-\frac{\beta x}{3}}\right) & \text{if } \beta > 0 \end{cases} \tag{19}$$

Here, q_L [L^2/T] represents the influx of eroded coarse sediment collected over a drainage-basin half-width of $x/3$, minus loss to abrasion over a travel distance equal to that width. Note that the width of the drainage basin at any point along x derives from differentiating (8) with respect to x, resulting in a width of $\frac{2}{3}x$. The channel is assumed to occupy the centerline of the drainage basin, so the length of tributaries entering the main channel at any point is equal to half of the total drainage basin width at that point, $\frac{1}{3}x$.

Our model does not explicitly handle the processes that deliver sediment from hillslopes to tributary channels; instead, we use γ to represent a fraction of the total eroded hillslope material that enters the channel as coarse sediment and thus is subject to grain attrition. In the case when $q_L = 0$, there is no lateral sediment supply; we conceptualize this case as a 'single-thread channel with no tributaries', which is explored more in the Section 3.9 and the supporting information.

3.8 | Sediment mass conservation

Sedimentation is the sum of processes that contribute to an increase in sediment thickness on the riverbed, minus those that degrade bed sediment thickness. Recalling (4), the sedimentation rate depends on the sediment influx and outflux, bedload losses to attrition, the generation of new coarse sediment via plucking, and lateral sediment inputs. We combine (10), (18), (15) and (19) into an integrated statement for sediment mass conservation. Note that plucking rate is multiplied by γ, which again represents the fraction of plucked material that actually becomes coarse bedload sediment:

$$\frac{\partial H}{\partial t} = -\frac{1}{(1-\phi)B}\left(\frac{\partial Q_s}{\partial x} + \beta Q_s - KIQS^{7/6}\alpha\gamma - q_L\right) \tag{20}$$

The terms in parentheses on the right represent sediment influx/outflux, attrition, plucking and lateral supply, respectively. Calculating sedimentation also requires a porosity factor, ϕ, and averaging across the valley.

3.9 | Analytical solution and nondimensionalization

Nondimensionalization is a useful practice that can reveal fundamental relationships in complex systems. It simplifies sensitivity analyses by reducing the number of parameters required to describe the full range of model behaviour. If an analytical solution exists, nondimensionalizing this single equation should reveal the fundamental, nondimensional parameter groups that control model behaviour.

We present an analytical solution for the special case of a single-thread channel with no tributaries where discharge and sedimentation are calculated only for the main channel (i.e., $Q = r\int B$ and $q_L = 0$). While this scenario is admittedly more limited than the full version of our model, it nevertheless provides insight into the structure and behaviour of the model and is useful as a tool to verify our numerical implementation. For simplicity, we also assume in this case that bedrock and sediment have the same abrasion properties, so $\zeta = \beta$. Given these conditions, the solution for equilibrium channel slope gradient is

$$S = \left[\frac{UB}{\left(\frac{1}{\frac{K_f}{\beta k_{Qs}}(1-e^{-\beta x})+1}\right)\beta I\left(k_{Qs}\left(1-\frac{1}{\frac{K_f}{\beta k_{Qs}}(1-e^{-\beta x})+1}\right)+\frac{K}{\beta}\right)}\right]^{6/7} Q^{-6/7} \tag{21}$$

The full derivation of (21), along with figures highlighting the performance of the analytical solution compared with the numerical model, can be found in Appendix B in the supporting information. We can nondimensionalize this analytical solution by nondimensionalizing several of our governing equations, which requires choosing scales for vertical length, horizontal length and time (Willgoose et al., 1991b). A

natural choice for vertical length scale exists in H^*, as it appears in the bed cover factor α (9). β is used for the horizontal length scale because it appears mathematically in cases of full sediment cover as well as partial bedrock exposure. To represent a time scale, there is a choice between two parameters that contain time: uplift rate and runoff rate. Of these, runoff rate is a good choice because it must be nonzero for erosion to occur. We define the characteristic time scale as $t_c = H_*/Ir$, which represents the duration needed for runoff to accumulate to a depth H_*. Including the intermittency factor, I, allows us to represent mean runoff rather than instantaneous runoff.

With these scales in mind, dimensionless dependent and independent variables are

$$\begin{aligned} H' &= H/H_* \quad \text{dimensionless sediment thickness} \\ \eta' &= \eta/H_* \quad \text{dimensionless height} \\ \eta_b' &= \eta_b/H_* \quad \text{dimensionless bedrock height} \\ x' &= \beta x \quad \text{dimensionless distance} \\ t' &= tIr/H_* \quad \text{dimensionless time} \end{aligned}$$

With length and time scales chosen, we are able to nondimensionalize our governing equations to arrive at the following nondimensional form of the analytical solution for the special case of a channel with zero tributary sediment or water inputs:

$$S = \left[\frac{B\beta \frac{U}{Ir}}{\left(\frac{1}{\frac{K_f}{\beta k_{Qs}}(1-e^{-x'})+1}\right)\left(k_{Qs}\left(1-\frac{1}{\frac{K_f}{\beta k_{Qs}}(1-e^{-x'})+1}\right)+\frac{K}{\beta}\right)} \right]^{6/7} x'^{-12/7} \quad (22)$$

where x' is dimensionless length, $x' = \beta x$. The full nondimensionalization can be found in Appendix C in the supporting information.

Examination of (22) reveals three dimensionless parameter groups and two dimensionless single variables that govern model behaviour: an uplift-runoff number (U/Ir), a width-abrasion number ($B\beta$), a plucking efficiency number (K/β), the sediment transport efficiency factor k_{Qs}, and the fraction of eroded material that becomes coarse sediment, γ. The full range of model behaviour can be expressed through varying these parameters; we conduct sensitivity experiments on four of these five numbers (Table 1), recognizing that because β appears in both the width-abrasion number and the plucking efficiency number, we can elucidate the impact of changing valley width, B, on the model indirectly through testing the plucking efficiency number.

3.10 | Model implementation and testing

Despite their astounding diversity, many rivers exhibit common forms and behaviours. As our model combines elements of both bedrock incision processes and alluvial transport processes, we will examine its ability to replicate morphologies associated with both bedrock and alluvial systems. When the incision rate is roughly uniform in space, bedrock-incising rivers typically exhibit an inverse relationship between slope and drainage area that can often be approximated as a power law. Furthermore, such channels usually show a positive correlation between gradient (normalized for drainage area) and the long-term average rate of downcutting (Lague, 2014). Meanwhile, rivers with gravel-alluvial morphology exhibit a systematic relationship between bankfull width and discharge, particularly when normalized by median grain size (Phillips et al.2022).

In the section below, we review our model's ability to reproduce these characteristic features, using four dimensionless parameter groups identified through nondimensionalization of the analytical solution to guide a sensitivity analysis. It should be noted that the analytical solution (21) does not include lateral sediment supply, while all results from numerical modelling experiments shown in the following sections do include this term; therefore, the dimensionless parameter

TABLE 1 Parameter suite used in sensitivity analysis.

Parameter group	Group name	Parameter varied	Default value	Tested values
$\frac{K}{\beta}$	Plucking efficiency	K	1×10^{-6} m^{-1}	1×10^{-7}
				3.2×10^{-7}
				3.2×10^{-6}
				1×10^{-5}
$\frac{U}{Ir}$	Uplift-runoff	r	5 m year^{-1}	1
				2.5
				7.5
				10
k_{Qs}	Sediment transport efficiency	k_{Qs}	0.041	0.021
				0.031
				0.051
				0.061
γ	Gravel fraction	γ	0.5	0.25
				0.375
				0.625
				0.75

Note: 17 runs are presented herein: one default run, and four runs for each of the four parameter groups.

groups serve as a guide to explore model behaviour in an organized framework, but do not make exact predictions about steady state conditions when $q_L > 0$. In the results below, the four dimensionless parameter groups are varied around a set of default parameter choices (Table 1) that have been selected based on a combination of empirical data and optimization of runtimes. Our model is implemented on a 1D grid with a total domain length of 50 km and grid spacing of 500 m. The model is forced with a constant rate of baselevel fall and is solved using a forward Euler finite difference scheme. For simplicity in evaluating the model's behaviour, we assume homogeneous bedrock and sediment. Some implications of imposing heterogeneity are explored in Section 4.

4 | RESULTS

4.1 | Slope-area scaling

River networks commonly exhibit an inverse relationship between slope and drainage area. This relationship is often described as a power law (Flint, 1974) of the form:

$$S = k_s A^{-\theta} \tag{23}$$

where A is drainage area, k_s is a steepness index (an area-normalized measure of stream gradient), and θ is a positive parameter often referred to as a concavity index, because its value describes the degree of longitudinal profile concavity (Whipple & Tucker, 1999). This type of scaling is so pervasive that it is considered a necessary criterion for incision models to replicate (Lague, 2014). Across a range of bedrock pluckability values, runoff rates, sediment transport efficiency and gravel fraction, our model predicts an inverse near-power law relationship between slope and area (Figure 3). By varying one parameter in each of our four dimensionless numbers, as outlined in Table 1, the model predicts changes in steepness in different parts of the channel profile (e.g., varying bedrock pluckability impacts steepness in the headwaters, while varying sediment transport efficiency impacts steepness in the downstream reaches); the locus of these effects reflects where in the profile sediment is providing a 'cover' effect to shield bedrock from erosion.

It is worth noting that our model does not predict uniform concavity, which contrasts with traditional formulations of the stream power incision model (Lague, 2014). Instead, examination of (21) reveals that there is a strong power law aspect embedded within the analytical solution, but the steady state profile also depends on the ratio of plucking to abrasion and the sediment transport efficiency—factors that do not appear in the stream power model. We posit that noisy field data are generally not sufficient to falsify the prediction that the slope-area relationship, while clearly an inverse one, can deviate from simple power law behaviour. Additionally, while changing bedrock properties leads to significant differences in steepness and concavity in the headwaters region (Figure 3a), drainage areas below $\approx 10^7 m^2$ in natural systems may be heavily influenced by nonfluvial processes (Lague, 2014), which leads to additional scatter in slope-area data when examining small drainage basins.

4.2 | Relationship between steepness and erosion rate

Channels typically become steeper as erosion rate increases; this is another trait so common that it is considered imperative for incision models to capture (Lague, 2014). Channel steepness can be examined by calculating a normalized steepness index, or by simply examining slope-area plots. Figure 3b demonstrates that channels become steeper as runoff rate decreases. While the parameter varied is not rock uplift rate, examination of the dimensionless uplift-runoff number (U/Ir; see Table (1)) demonstrates that increasing runoff rate, r, has an equivalent effect on model behaviour as decreasing rock uplift rate, U, which in turn decreases the steady state erosion rate. Therefore, we can examine how channel steepness changes with variable runoff rates as a proxy for how channel steepness changes with

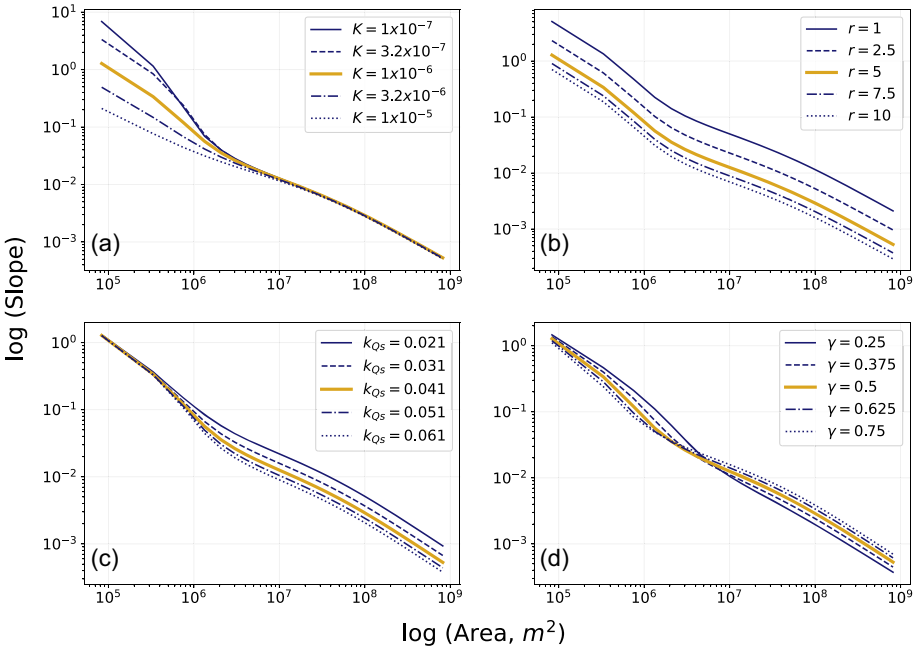

FIGURE 3 Variations in bedrock pluckability (a), runoff rate (b), sediment transport efficiency (c) and gravel generation rate (d) lead to changes in steepness in the different parts of the channel profile. The gold line is the same in each plot, representing the default model run that uses all the default parameter values outlined in Table 1 and in Appendix A: Notation in the supporting information. [Color figure can be viewed at wileyonlinelibrary.com]

erosion rate. Figure 3 shows that channels become steeper when runoff rate is low; because runoff and rock uplift are inversely related in our dimensionless parameter groupings, this implies that channels become steeper when uplift rate is high.

4.3 | Near-threshold geometry

Phillips et al. (2022) present a composite dataset of hydraulic geometry for over 1600 rivers across six continents. These data demonstrate that many alluvial channels, occurring across a wide range of scales, hydro-climates, sediment supply regimes and bedrock geology, have scaling relationships between width, depth, slope and discharge that are consistent with the prediction of near-threshold theory (Phillips & Jerolmack, 2016), albeit with variability in the estimated bankfull Shields stress. Phillips and Jerolmack (2016) argued that, because some 'bedrock-influenced' and 'mixed alluvial-bedrock' channels also show scaling consistent with near-threshold theory, the basic principle behind near-threshold theory may also apply to at least some bedrock-incising channels. This hypothesis motivates one of the driving questions behind our model: Is it possible for a river to exhibit both bedrock incision and near-threshold geometry?

Consider the case of the upper Colorado River: over roughly 1000 km from western Colorado to just above Lees Ferry, AZ, cosmogenic burial dating on terraces has revealed bedrock incision rates on the order of 100 m/Ma (Darling et al., 2012). In the same vicinity, spanning roughly 250 km from western Colorado to Moab, UT, Pitlick and Cress (2002) documented bedrock-influenced ('quasi-alluvial') reaches that showed bankfull Shields stresses between approximately 0.03 and 0.09—values that were similar to those found in fully alluvial reaches of the channels and that are consistent with near-threshold theory. Together these studies demonstrate bedrock incision over million-year timescales and consistency with near-threshold theory, even in reaches that presently have bedrock exposure. This certainly does not mean that all bedrock-incising rivers have a bankfull Shields stress close to threshold, or that the concept of bankfull flow is meaningful for all bedrock-incising rivers, but it does demonstrate the existence of at least one bedrock-incising near-threshold river. Other examples of channels contained within the Phillips et al. (2022) dataset that exhibit near-threshold behaviour and whose geologic contexts imply long-term bedrock incision include Tonto Creek near Roosevelt, AZ ($\tau_b^* \approx 0.03$, $D_{50} \approx 0.02$ m, incised into Proterozoic metavolcanic rocks); South Fork Poudre River near Rustic, CO ($\tau_b^* \approx 0.01$, $D_{50} \approx 0.15$ m, incised into Proterozoic crystalline rocks); Lochsa River, ID ($\tau_b^* \approx 0.03$, $D_{50} \approx 0.15$ m, incised into metamorphic and igneous rocks); Sand Run, WV ($\tau_b^* \approx 0.02$, $D_{50} \approx 0.12$ m, incised into various sedimentary units); Rio Mameyes near Sabana, PR ($\tau_b^* \approx 0.06$, $D_{50} \approx 0.15$ m, incised into serpentine and basalts); and Rogue River near Agness, OR ($\tau_b^* \approx 0.07$, $D_{50} \approx 0.04$ m, incised into accreted sedimentary terranes and intrusive crystalline rocks). While the bankfull Shields stress is low for some of these examples, which may reflect methodological issues with grain sampling or bankfull geometry measurements, or simply large uncertainty bounds associated with such estimates, these bedrock-incised streams are not much more powerful in terms of their Shields stress than near-threshold theory would predict for gravel-bed alluvial rivers. While we don't presently know how common it is for bedrock-incising streams to exhibit near-threshold style adjustment, the fact that at least some subset of bedrock-incising channels appear to self-adjust raises the question of how such behaviour would manifest in long-term profile evolution, and to what extent that predicted behaviour is consistent or inconsistent with observations. Here, we test whether our model, which includes bedrock incision as a steady state condition, can also replicate near-threshold channel geometry.

We filter the dataset from Phillips et al. (2022) to examine only those channels whose median grain size is equal to or coarser than 2 mm and can thus be considered 'gravel-bedded'. The vast majority of these channels have drainage area greater than 1 km^2 and slope less than 0.04. While the exact limitations of near-threshold theory may not be known, these metrics may provide a rough initial estimate of the bounds of the theory's applicability. By plotting channel width, depth and slope against discharge, we see that strong correlations between width and discharge and between depth and discharge emerge even when the original dataset is filtered for coarse sediment. And while there is a higher degree of scatter in the slope data, we nevertheless can observe an inverse correlation between slope and discharge. When we add our modelled channels to these data, we find that the model is capable of producing channels with hydraulic geometries similar to global trends; this behaviour is consistent for a range of bedrock properties, runoff rates, sediment transport efficiency and gravel fractions (Figure 4).

However, this behaviour is not inevitable: for example, if we envision a case in which grain attrition is limited such that the characteristic length scale for attrition is much longer than the length of the fluvial profile (e.g., if $1/\beta = 2 \times 10^5$ m while $x = 10^5$ m), then the resulting channel becomes overly wide, shallow and steep, and the downstream reach exhibits a near-constant slope gradient (Figure 5). The straight profile is a consequence of the linear dependence of sediment transport rate on bankfull discharge (Equation 10), and it is the expected morphology when runoff rate is uniform and attrition is minimal. It reflects a system in which the downstream growth in bankfull discharge is balanced by downstream growth in sediment load. Such scenarios help define the limitations of model applicability, demonstrating that near-threshold behaviour is not guaranteed to arise simply because of the model formulation and that grain attrition may be a fundamental ingredient in producing near-threshold river profile geometries.

4.4 | Transport-limited and detachment-limited erosion

In addition to replicating expected fluvial features and geometries, our model is consistent with previous erosion-deposition models in its ability to represent a continuum between more detachment-limited and more transport-limited erosional styles (Beaumont et al., 1992; Davy & Lague, 2009; Shobe et al., 2017). We follow the approach of Sklar and Dietrich (2004) in relating bed cover fraction to transport rate, assuming that

$$Q_s = (1-\alpha)Q_c \tag{24}$$

Because α is defined as the bedrock exposure fraction, $(1-\alpha)$ is the bed cover fraction. Q_c is transport capacity $[L^3/T]$ defined as the

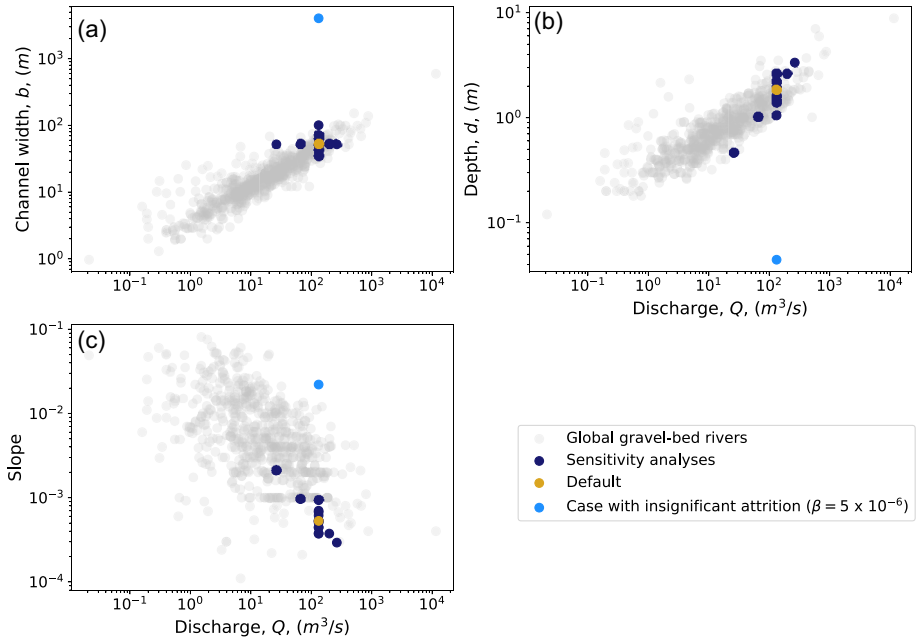

FIGURE 4 17 model runs with bankfull discharge (16 sensitivity analysis runs and the default model), shown in dark blue, produce geometries consistent with a global dataset of bankfull alluvial river widths, depths and slopes. Each point represents conditions at the downstream-most channel node. Modelled channel slopes generally skew towards low slope values due to our choice of a relatively small D_{50} (1 cm). Not all model runs fit these trends; an example outlier, in which grain attrition is very low, is plotted in light blue. Figure modified after Phillips *et al.* (2022). [Color figure can be viewed at wileyonlinelibrary.com]

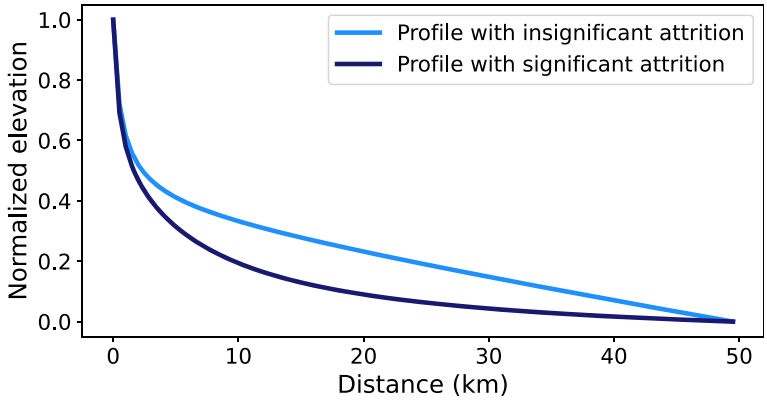

FIGURE 5 Examples of profiles developed when attrition is significant (dark blue line; $\beta = 5 \times 10^{-4}$) versus insignificant (bright blue line; $\beta = 5 \times 10^{-6}$) compared with the length of the channel profile (10^5). When attrition rate is small relative to the length of the channel, coarse sediment can be generated by cannot be worn away. This causes the ratio of transport to capacity (Q_s/Q_c) to remain constant, rather than tapering off slightly downstream as seen in Figure 6; this is reflected in the creation of straight profiles, which is the channel's response to transporting sediment supply that increases linearly downstream with discharge. [Color figure can be viewed at wileyonlinelibrary.com]

sustained transport rate that occurs under an unlimited supply of bed sediment of a given size, density and shape. When α is zero, bedrock in the riverbed is entirely shielded from erosion and sediment transport, Q_s, equals transport capacity, Q_c. Therefore, the bed cover fraction $(1-\alpha)$ is equivalent to the ratio between sediment transport rate and transport capacity, Q_s/Q_c. By plotting bed cover against distance, we can examine how the model shifts from more detachment-limited behaviour to more transport-limited behaviour along stream (Figure 6).

The steady solutions imply that the ratio of sediment transport to transport capacity (Q_s/Q_c) should increase rapidly downstream from the channel source as sediment is generated through plucking in the main channel and delivered to the mainstem by tributaries. All experiments also exhibit steady-state behaviour in which the ratio of transport rate to transport capacity tapers off slightly after reaching an initial peak. This occurs as transport rate decreases relative to transport capacity: while transport capacity continues to increase downstream with discharge, transport rate slows as bedload in transport is lost to attrition.

We find that parameter groups that directly affect the mass of bedload material present, such as the bedrock pluckability and gravel fraction, exert the greatest control on the transport to transport capacity ratio, Q_s/Q_c. Varying runoff has no effect because both transport rate and transport capacity depend linearly on discharge: transport rate is given by (10), while transport capacity is simply equivalent to (10) when $\alpha = 0$. This relationship demonstrates that any change in transport capacity resulting from altered discharge will be met with an equivalent change in transport rate, all else being equal. While changing the sediment transport efficiency can alter the ratio of transport rate to transport capacity, these changes are very minor, in part because the sediment transport efficiency is only varied over a small range of values due to its dependence on fixed quantities such as sediment and water density and gravitational acceleration.

The model's ability to perform across a range of criteria related to both bedrock-incising and alluvial river systems demonstrates that it is possible to create a model that (1) reproduces fluvial forms consistent with predictions from the stream power incision model (associated with bedrock-incising channels), (2) adheres to a realistic hydraulic geometry for alluvial rivers, and (3) erodes bedrock at steady state even while transporting sediment at near-transport capacity. Note that when the model is forced by rock uplift, bedrock erosion will always be part of the steady state behaviour. Therefore, steady state fluvial behaviour may approach a fully transport-limited state, but cannot achieve this condition entirely. Interestingly, this implies persistent bedrock exposure occurs in the channel over tens of kilometres. While this may seem contrary to observation, substantial bedrock

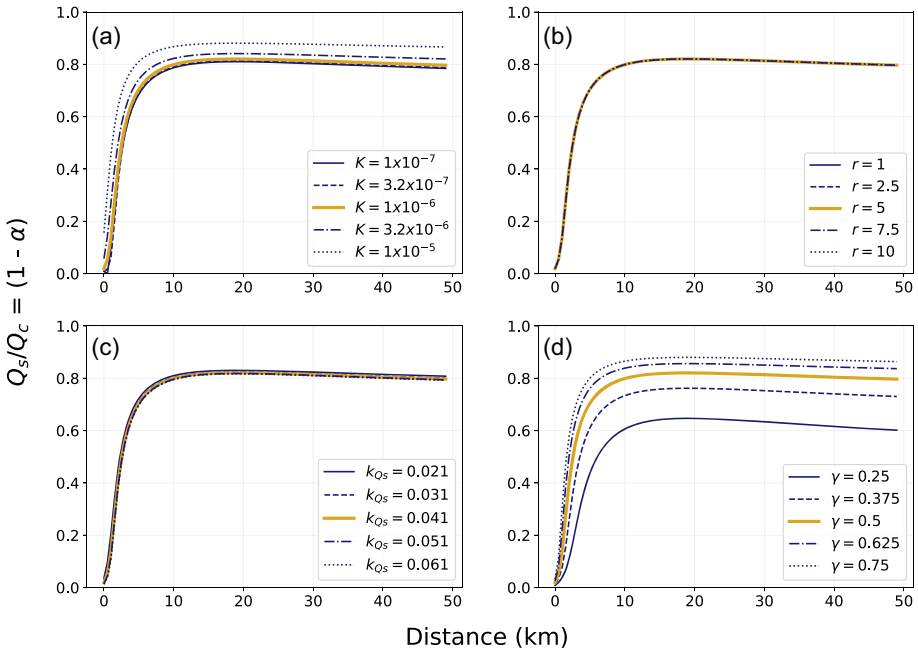

FIGURE 6 More pluckable (higher K value) bedrock pushes the model towards more transport-limited behaviour (a), while increasing or decreasing runoff has no effect because transport rate increases linearly with discharge (b). Changing sediment transport efficiency has little effect over the range of values tested (c); the value of k_{Qs} lumps together factors including gravity, excess shear stress and sediment and water density. As these values should not vary greatly, it is appropriate to only test k_{Qs} over a small range of values. Varying the fraction of eroded material that becomes coarse sediment has the greatest effect on the ratio of transport rate to transport capacity (d). [Color figure can be viewed at wileyonlinelibrary.com]

exposure has been documented tens to hundreds to kilometres from the headwaters, and persistently outcropping for tens of kilometres, on rivers including the Colorado (Pitlick & Cress, 2002) and the Peikang (Yanites et al., 2010, Yanites et al., 2011); bedrock exposure has even been documented on large lowland rivers, such as the Mekong and the Ganga through Bangladesh (Meshkova & Carling, 2013), though there is often insufficient data to constrain the extent over which these outcrops persist. Moreover, the results presented here encourage us to think of 'detachment-limited' and 'transport-limited' as endmembers on a spectrum of fluvial behaviour. The high ratio of transport to capacity exhibited in our model runs (Figure 6), combined with the channel geometries showcased in Figure 4, suggest that our channels are strongly adjusted to transport sediment even while incising bedrock. These channels may therefore be best described as 'transport-dominated', even though the detachment of rock has some influence on profile morphology. Fully transport-limited behaviour could occur under cases of temporally nonuniform rock uplift, or with a substrate composed entirely of sediment rather than rock.

5 | DISCUSSION

Our results demonstrate that the model is broadly equipped to evolve fluvial profiles under conditions of bedrock incision and sediment transport. Below, we discuss the limitations of the model and its place amongst theory and observations of fluvial systems.

5.1 | Improvements and changes to fluvial modelling and theory

The model described here generally fits a framework of fluvial features predicted by both observation and theory. However, where it deviates from this framework gives useful insight into areas where our longstanding assumptions may be reexamined.

5.1.1 | The slope-area relationship and the effects of sediment on concavity

The relationship between slope and area in river profiles with spatially uniform erosion rates has long been described as a power law (23), where θ is a constant with value close to 0.5. This idea is grounded in extensive field observations (e.g., Flint, 1974; Tarboton et al., 1989) and is consistent with stream power model predictions for steady state river profiles. However, field slope data are notoriously noisy, and concavity values are obtained by fitting this data with a straight line in log-log space. Our model predicts that concavity is not constant along profile, but rather fluctuates over a small range at steady state. We posit that the extent of this fluctuation is likely indistinguishable from noise inherent in slope data. This represents a significant departure from theory and holds implications for our evaluations of 'steady state' criteria in modelling profile evolution, as well as for distinguishing amongst hillslopes, colluvial channels and alluvial channels in slope-area data (e.g., Montgomery & Foufoula-Georgiou, 1993; Willgoose et al., 1991c). The reason behind our model's nonuniform prediction of concavity can best be understood by examining how the model behaves under a range of sediment hardness conditions. Our findings apply to systems carrying uniform sediment across lithologically homogeneous terrain. However, real landscapes are often highly heterogeneous, and this heterogeneity in bedrock leads to heterogeneity in sediment characteristics, as well. Our model allows one to explore how interactions between bedrock and sediment comprising different lithologies may affect the shape of a steady state profile.

Field studies have demonstrated that rivers whose bedload is hard relative to the local riverbed substrate tend to be steeper than channels on the same substrate that lack tough bedload clasts (Duvall et al., 2004; Finnegan et al., 2017; Johnson et al., 2009; Lai et al., 2021). To test whether our model is consistent with this behaviour, we compare the steepness of profiles with sediment akin to the bedrock substrate ($\beta = \zeta$) versus those with sediment that is either harder ($\zeta > \beta$) or softer ($\zeta < \beta$) than the bedrock underlying the profile (Figure 7). Our model assumes the hypothesis that sediment cover

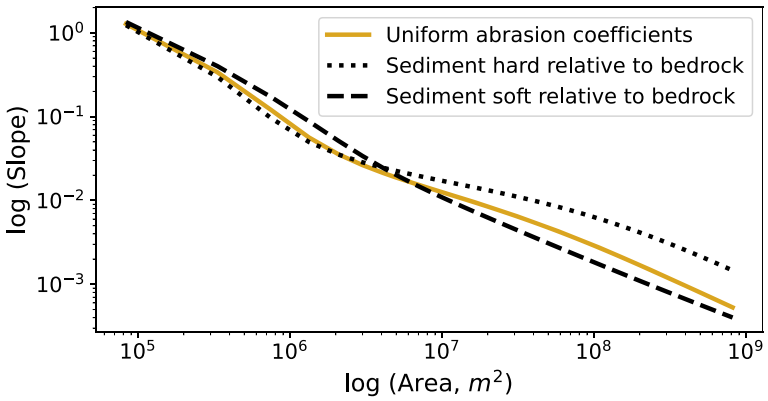

FIGURE 7 When sediment is hard relative to the underlying bedrock (less abradable; $\beta < \zeta$), channels develop shallower slopes in their upstream reaches because the low concentration of sediment in transport (Q_s/Q_c), combined with the persistence of that sediment, allows it to be an effective tool that abrades the riverbed and promotes increased bedrock erosion. However, these channels also develop steeper downstream profiles because, as sediment concentration bulks downstream, increased sediment shielding of bedrock requires the channel must be steeper to keep pace with rock uplift (dotted line). When sediment is softer than the underlying bedrock ($\beta > \zeta$), the opposite is true: upstream profiles are steeper because the soft sediment in transport is less effective at lowering the bedrock elevation through abrasion, while downstream profiles are less steep because more rapidly abrading sediment allows bedrock erosion to be more efficient, thus requiring lower slopes to keep pace with rock uplift (dashed line). The gold line represents our default model case where sediment and bedrock have the same abrasion/attrition coefficients. [Color figure can be viewed at wileyonlinelibrary.com]

can reduce erosional efficiency and, within the framework of this hypothesis, provides a physical explanation for the relationship between sediment hardness, sediment cover and channel slope.

When sediment is hard relative to the riverbed, we find that steady state channels are less steep in their headwaters, and more steep in their downstream reaches, when compared with channels whose bedrock and sediment have comparable abrasion coefficients. The inverse is true when sediment is soft relative to the underlying bedrock: these channels are steeper in their headwaters and less steep in their downstream reaches. This result can be understood in terms of the 'tools and cover' effect (Sklar & Dietrich, 1998). Take the case with relatively hard sediment as an example: when sediment is more resistant to grain attrition, a small number of clasts in transport in the headwaters can enhance bedrock erosion by acting as 'tools' that abrade the riverbed. Thus, channel slopes are lower in the upstream reaches because bedrock erosion is more efficient. However, as more sediment enters the bedload with distance downstream, it increasingly acts as 'cover', which reduces the efficiency of the model's bedrock erosion processes. This forces the model to maintain higher downstream slopes in order to transport sediment while also achieving the steady state bedrock erosion rate. Therefore, the non-uniform concavity predicted by our model can be understood to reflect a transition from a 'tools-dominated' channel to one that is 'cover-dominated'. It should be noted that the 'tools-dominated' model domain occurs over small drainage areas in the headwaters, where near-threshold channel theory may break down either because rivers in such small drainages don't develop substantial floodplains and experience more bank confinement, or because bedrock incision and sediment transport in these drainages are influenced by debris flows and other colluvial processes (Montgomery & Foufoula-Georgiou, 1993; Campforts et al., 2022). This phenomenon may explain why the examples we find in the literature of sediment impacting channel slopes have focused instead on how sediment can lead to increasing channel steepness. Note also that if the grain attrition length scale is sufficiently short relative to the length of the channel or reach of interest, all sediment generated through plucking can be worn away so rapidly that the model essentially becomes the stream power incision model: under these conditions, not only is channel steepness reduced, but concavity nears a constant value as predicted by the stream power model.

5.1.2 | Scale-dependence of rock strength and implications for bedload abundance

This model adds nuance to ideas about how profile evolution and fluvial behaviour change in response to changing bedrock and sediment characteristics. Stream power theory lumps multiple processes into a single erodibility coefficient; presumably both plucking and bedrock abrasion are encapsulated in this coefficient, yet the material properties that influence the effectiveness of these two processes are somewhat distinct. When plucking or abrasion are explicitly parameterized in the literature, plucking is typically related to macroscale features such as submeter joint spacing (Whipple et al., 2000), while abrasion rates are typically related to rock tensile strength (Sklar & Dietrich, 2001, 2004; Chatanantavet & Parker, 2009). Tensile strength measurements provide information about the strength of a rock sample; they do not capture field-scale complexity in rock properties such as the presence of faults and joints. Moreover, tensile strength measurements made on hand samples reflect the strength of sediment in transport, which may differ from the local bedrock substrate if the sediment is sourced from a different geologic unit. Our model provides greater insight to the processes controlling fluvial evolution by treating plucking, abrasion and attrition separately.

An example of a case in which considering these processes separately can be useful is found by critically examining Figure 6a. This plot shows that if we increase K to represent bedrock becoming more erodible via plucking (which could represent, e.g., extensively fractured as opposed to massive bedrock), the system moves towards more transport-limited behaviour. This result is unsurprising: because plucking generates bedload sediment, more pluckable bedrock leads to more sediment in transport. However, nondimensionalization of

the model reveals that the relationship between plucking and attrition is K/β (see Section 3.9 and Table 1), implying that decreases in K should have the same effect on model behaviour as increases in β; it follows that increasing the attrition coefficient, which should represent rock susceptibility to erosion at the grain scale, will have the opposite effect as increasing the bedrock pluckability. This is because increasing the bedrock plucking rate (K) leads to the generation of new bedload sediment, while increasing the sediment attrition rate (β) leads to the more rapid destruction of existing bedload sediment.

It should be noted that this model does not differentiate between a median grain size generated in-channel and the grain size delivered from surrounding hillslopes, despite the latter exerting a large degree of control on channel slope (Sklar & Dietrich, 2001; Sklar et al., 2017). Differences in physical processes generating sediment in-channel through plucking and abrasion, versus sediment production on hillslopes by processes such as freeze-thaw cycling and fracturing by roots, are not explicitly represented. Rather, this model treats the hillslope contribution indirectly by multiplying the channel erosion rate by a factor (γ) representing the fraction of eroded material that becomes coarse sediment (see Equation (19)). Nonetheless, the simple experiment highlighted by Figure 6 demonstrates that fluvial behaviour responds in a complex way to variations in rock strength, and researchers with interest in modelling structurally or lithologically heterogeneous settings should account for the different scales of rock strength that may be relevant in parameterizing their models.

5.1.3 | Channel widening under high supply conditions

Recall from Section 4 that the model predicts a steady state slope-area relationship governed by a transition from a 'tools-dominated' profile to one that is 'cover-dominated'. In addition to causing our model to deviate from having uniform concavity, this effect has some interesting consequences for channel width.

Stream power models typically impose a fixed relationship between channel width and discharge (commonly one in which channel width increases as the square root of discharge), an empirical relationship derived from observations of alluvial channels that also appears to apply to channels with partially alluviated beds (Hack, 1973; Leopold & Maddock, 1953). If we accept that this relationship ought to be extended to bedrock-incising channels, then it implies that, all else being equal, bedrock-incising channels should have a greater erosion potential in a narrower channel because the hydraulic power and frictional force are concentrated over a smaller channel area. Moreover, it has been hypothesized that a bedrock-incising channel might tend to narrow in response to increased gradient because the same discharge can be conveyed with a reduced width and depth (Finnegan et al., 2005). Several case studies have corroborated this prediction, finding that channels may narrow and steepen to increase erosional efficiency following tectonic perturbations (Whittaker et al., 2007), in response to spatially variable uplift rates (Lavé & Avouac, 2001), and, on shorter timescales, to digest large volumes of landslide-produced sediment (Croissant et al., 2017). However, the exact processes that control this relationship have not been fully explored: for example, an inverse relationship between channel gradient and channel width could arise from bedrock confinement (perhaps reflecting faster incision under a steeper gradient), or could result from changes in the grain size distribution fed to the channel from surrounding hillslopes (a tectonic perturbation that steepens a channel might also deliver coarser sediment; the near-threshold mechanism would then predict a narrower channel under coarser bed and bank sediment, all else equal).

Amongst channels that conform to near-threshold predictions for hydraulic geometry, however, Equation (6) stipulates that width should increase with increases in both discharge and slope. The consequence of this relationship is that, for any given position (i.e., discharge rate, Q) in the river profile, our modelled channels are widest when they are also steepest. Recalling that channel steepness increases with sediment supply in 'cover-dominated' reaches (Figure 7), our model predicts channels will widen under conditions of high sediment supply for all drainage areas outside of small headwaters catchments. This is somewhat counterintuitive: we might expect a channel to adjust via both narrowing and steepening in order to maximize unit stream power to most efficiently process a high sediment supply, yet such an adjustment would be incompatible with the assumption of constant bankfull bed shear stress.

While field observations are limited, there is some evidence for bedrock-incising channels that might be well-represented by the near-threshold prediction of widening under high supply conditions. Recent work from Taiwan has documented that channel widths on Taiwan's southern peninsula vary systematically with steepness: the steepest channels tend to be the widest. Taiwan is subject to rapid tectonic uplift and channel incision into bedrock (Yanites et al., 2010); the extreme uplift rates and precipitation patterns found on the island also lead to abundant landsliding, which provides high sediment supply to mountain streams (DeLisle et al., 2022). Yanites et al. (2018) found that the steepest channels on Taiwan's Hengchun Peninsula received the most sediment as a consequence of widespread landsliding after an intense rainfall event, particularly focused in the upstream reaches of their catchments, corresponding to these channels being positioned in valleys with the highest hillslope gradients. Prior to the precipitation event, these steepest channels were already the widest found in the study area, and they experienced the most post-event widening. The authors also found that, while channel width increases with distance downstream, channel wideness (width normalized by drainage area) slightly decreases with distance downstream in the steepest channels. These observations led Yanites et al. (2018) to conclude that channel morphology (width and slope) in Taiwan is strongly controlled by sediment supply and that large supply events such as typhoons may exert a long-term control on the landscape evolution of Taiwan; further work in the area has corroborated this hypothesis, finding that channel slopes in Taiwan are mostly adjusted to transport sediment (Lai et al.2021).

This model predicts widening under high sediment supply conditions—a prediction that appears to be consistent with some field areas, such as Taiwan's southern peninsula. However, it is also true that channel narrowing to process large amounts of sediment has been documented elsewhere (e.g., Croissant et al., 2017). One explanation for the differences in observed channel response to sediment loading is that some channels conform to near-threshold theory, and others do not. A more nuanced explanation, however, is that median grain diameter (D_{50}) is inversely proportional to channel width in the near-threshold framework (6). Large sediment delivery events, such as

landslides, could mobilize larger grains that temporarily raise the D_{50} value, resulting in channel narrowing. Our model does not make this prediction because we assign only one grain diameter to the gravel fraction, so (6) is effectively only sensitive to changes in slope that result from increasing or decreasing the total amount of bed cover. Phillips and Jerolmack (2016), however, recognized that channels have two avenues of adjustment to maintain near-threshold behaviour: width adjustment and sediment sorting. It is possible that the observed discrepancies in channel response to sediment loading are related to whether or not that sediment loading event results in a significant shift in D_{50}. The fact that this model can only reproduce one type of adjustment to maintain near-threshold behaviour represents a limitation that could be the focus area for future improvements.

Channel widening under high supply conditions remains an area in need of further study; however, this model presents a mathematical framework with which to interpret the conditions that lead to widening and steepening in sediment-laden channels and allows us to make predictions about which parts of a river system may be primarily adjusted to incise bedrock and which parts are adjusted to transport sediment.

5.2 | Model limitations

Our model evolves fluvial profiles through plucking and abrasion of bedrock in near-threshold channels. Near-threshold geometry is maintained by assuming that the channels have at least one mobile bank capable of instantaneous lateral adjustment in response to changing sediment transport and discharge conditions. While lateral adjustments in response to sediment load are thought to proceed rapidly in near-threshold channels (Phillips & Jerolmack, 2016), this effect is not truly instantaneous but rather reflects a statistical average around that are fluctuations influenced by floods of varying magnitude and duration. Furthermore, use of a critical Shields stress based only on sediment median diameter neglects the potential effects of vegetation, which can play a large role in stabilizing banks (e.g., Arcement & Schneider, 1989; Montgomery & Buffington, 1997). This assumption means that the model tends to over-predict width in channels with heavily vegetated banks, but given that our model is capable of reproducing hydraulic geometries similar to those of real-world alluvial channels, this simplification does not appear to invalidate our analysis to first-order. However, higher-order complexity of real-world channels, such as sinuosity and lateral migration timescales, are not captured here. This limits the applicability of our model to studies in which the primary focus is on net landscape lowering and longitudinal valley form, as opposed to floodplain evolution or valley widening. Our model also ignores the existence of true bedrock confinement, such as bedrock-walled canyons that may coexist with gravel-bed rivers. In such cases, the processes that control lateral migration and valley widening may be fundamentally different from the near-threshold channel response that our model simulates. For example, channel adjustment in bedrock-confined settings may involve undercutting of cliffs, which leads to large sediment delivery events (e.g., rockfalls), the debris from which must be evacuated before further width adjustment or incision can occur (e.g., Fuller, 2014, Shobe et al., 2016). This is an active research frontier with important implications for landscape evolution modelling that are not captured in our formulation. However, our results call attention to the importance of bedload persistence in shaping river profiles and may therefore be useful in coupling processes like bedrock valley widening via undercutting with longitudinal profile evolution (e.g.,Langston & Tucker, 2018).

We simplify the treatment of sediment in our river channel. By treating only two size classes (gravel and fines), we ignore hydraulics specific to sand-bed rivers and also neglect nuances such as how the presence of sand can influence the gravel transport rate, for example, by lowering form drag associated with gravelly riverbeds (Wilcock et al., 2001). Although our model is capable of assigning different abrasion coefficients to the sediment and channel bedrock, sediment in our model has uniform characteristics. However, field studies have demonstrated that clast density, which reflects source rock lithology, plays an important role in controlling both streamwise changes to bedload composition, and the total abrasion rate of the bedload (Pfeiffer et al., 2022). While our model currently does not allow for heterogeneous grain populations, this is a potential direction for future improvement. Moreover, a thorough understanding of the 'effective' abrasion coefficient for a population of heterogeneous grains represents a knowledge gap that could be bridged in the laboratory, the field, or both.

Additional simplification of the sediment load comes in our assumption that only total bedload volume, and not median grain size, attenuates downstream via grain attrition. If we were to implement this model to reflect diminishing D_{50} downstream, our channel width relation given by (6) indicates that we would see enhanced stream widening with distance downstream. As discussed in Section 4 5.1.3, the choice to assign a single grain size to the gravel fraction also means that the model is not able to replicate any sediment sorting or selective transport processes, which is one way that channels adjust to maintain near-threshold behaviour (Phillips & Jerolmack, 2016). In addition to providing an avenue for near-threshold channel adjustment, sediment sorting and downstream fining also exert a control on long-profile evolution and basin-scale landscape morphology (e.g., Gasparini et al., 1999, 2004) Creation of a model that includes multiple grain sizes in the gravel fraction and that allows for size reduction of clasts in transport with downstream distance would represent a significant improvement. Such an improvement would likely result in a more realistic and nuanced width-discharge relationship and may allow for more varied channel response to sediment loading.

We have chosen to make several simplifications in our treatment of shear stress and roughness in our modelled channels, which come to bear on the model's sediment transport function. We use a single value of 0.0495 for τ_c^*, the critical Shields stress, which accounts for shear stress partitioning between grain mobilization and form drag (Meyer-Peter & Müller, 1948; Wong & Parker, 2006). In assuming a constant value of τ_c^*, we also assume that gravel-bedded channels obey the commonly observed, but by no means universal, ratio $\tau_b^*/\tau_c^* \approx 1.2$; in reality, research has shown that the Shields number varies with sediment supply (Pfeiffer et al., 2017) and the rearrangement of bedforms associated with seasonal flooding, and steep upland rivers are especially sensitive to this effect (Masteller et al., 2019). Additionally, field data suggests that the critical Shields number tends to be slope-dependent and is higher in steeper, shallower flows (Rickenmann, 2001; Rickenmann & Recking, 2011). While correction factors have been proposed (e.g., Ferguson, 2012),

we have chosen to use a simpler formulation in which we treat this value as constant. Additional simplifications can be found embedded within (6), in the factor k_b, which includes a calculation of flow velocity using the Manning–Strickler equation (see eqs. 10–12, Wickert & Schildgen, 2019). In this formulation, the characteristic roughness scale depends only on median grain size. Wickert and Schildgen (2019) defend this choice by pointing out that in gravel-bed rivers, the clasts themselves are the main source of roughness. However, roughness is a dynamic feature that can change with the rearrangement, creation and destruction of bedforms; these changes alter flow velocity and can contribute to the maintenance of critical flow in steep mountain channels (Grant, 1997). While we assume a constant roughness value in this model, it would be relatively straightforward to extend the formulation to incorporate a modified representation of roughness that varies with slope, such that an upper limit of unity is imposed for the Froude number.

Finally, we have chosen to limit our model analysis in this paper to the steady state condition, as our main goal has been to demonstrate the ability of a model to synthesize behaviours of 'bedrock' and 'alluvial' channels while producing broadly realistic fluvial forms. Current limitations to studying transient cases with this model include that (1) we explicitly set drainage basin geometry to calculate the length of tributary channels and (2) we assign the instantaneous main-channel erosion rate to all incoming tributaries: as such, this model does not allow for tributaries to be out of equilibrium with the main channel. However, the transient response of a sediment-influenced, bedrock-incising channel profile has been shown by Gasparini et al. (2007) to depend strongly on the timing and supply of sediment throughout the drainage system; a two-dimensional formulation is therefore required to properly represent transience. This model could be scaled up to run on a 2D grid, which would allow for an improved representation of basin-scale disequilibrium and thus would be more suited to represent transient responses; computational analysis and implementation of a two-dimensional model represents an opportunity for future work.

Despite these limitations, our model captures several key elements of reality that have been missing from previous models for river longitudinal profile evolution. This model is especially applicable to modelling gravel-bed rivers in which the channel length is large relative to the sediment attrition length scale, such that grain attrition becomes an important process in setting channel geometry. Testing and refining this model will require applying it to settings with more complex uplift and discharge histories and studying its ability to capture transient forms associated with dynamic forcing. This model also provides an avenue for exploration of questions relating to the role of sediment in setting channel width and steepness; in order to sufficiently address such questions, we will need to pay special attention to noting bedload characteristics (size, tensile strength, lithologic distribution) in tandem with hydraulic measurements such as slope, width and depth.

6 | CONCLUSIONS

By combining bedrock erosion, sediment transport and modification of sediment load through attrition, we have arrived at a model that captures behaviours of bedrock rivers while reproducing morphologies consistent with alluvial channels. Our mathematical formulation demonstrates that near-threshold models can be suitable for bedrock-incising rivers and that rivers whose behaviour falls near a 'transport-limited' condition can incise bedrock over long time periods. Future use cases for this model include the study of climate pulses on channel profile development, such as glacial/interglacial cycles where sediment supply fluctuates over long timescales; the role and fate of sediment in extreme sedimentation events, such as landslides; and channel development in lithologically heterogeneous terrain.

AUTHOR CONTRIBUTIONS

Vanessa Gabel contributed to the conceptualization, methods development, investigation, software development and writing of this manuscript. Gregory Tucker contributed to the conceptualization, funding acquisition, methods development, software development, supervision and editing of the manuscript. Benjamin Campforts contributed to the methods development, software development and editing of the manuscript.

ACKNOWLEDGEMENTS

This work was supported by the US National Science Foundation (2104102, 2100702, 2148762 and 1822062) and NASA (80NSSC22K0465).

CONFLICT OF INTEREST STATEMENT

The authors declare no conflicts of interest.

DATA AVAILABILITY STATEMENT

Source code to run the model, as well as parameters used to produce all model runs showcased in this manuscript, can be found on Github here.

ORCID

Vanessa Gabel https://orcid.org/0009-0006-1209-9636
Gregory E. Tucker https://orcid.org/0000-0003-0364-5800
Benjamin Campforts https://orcid.org/0000-0001-5699-6714

REFERENCES

Arcement, G.J. & Schneider, V.R. (1989) Guide for selecting Manning's roughness coefficients for natural channels and flood plains. In 2339, USGPO For sale by the Books and Open-File Reports Section, US Geological Survey.

Attal, M. & Lavé, J. (2006) Changes of bedload characteristics along the Marsyandi River (central Nepal): Implications for understanding hillslope sediment supply, sediment load evolution along fluvial networks, and denudation in active orogenic belts. In: Willett, S. D., Hovius, N., Brandon, M. T., Fisher, D. M. (Eds) *Tectonics, climate, and landscape evolution*, Geological Society of America, pp. 143–171. Available from: https://doi.org/10.1130/2006.2398(09)

Attal, M. & Lavé, J. (2009) Pebble abrasion during fluvial transport: Experimental results and implications for the evolution of the sediment load along rivers. *Journal of Geophysical Research: Earth Surface* 114(F4), 1–22. Available from: https://doi.org/10.1029/2009JF001328

Beaumont, C., Fullsack, P. & Hamilton, J. (1992) *Erosional control of active compressional orogens*. In: McClay, K. R. (Ed.) Thrust tectonics, 1st edition, New York: Chapman and Hall, pp. 1–18.

Buffington, J.M. & Montgomery, D.R. (1997) A systematic analysis of eight decades of incipient motion studies, with special reference to gravel-

bedded rivers. *Water Resources Research*, 33(8), 1993–2029. Available from: https://doi.org/10.1029/96WR03190

Campforts, B., Shobe, C.M., Overeem, I. & Tucker, G.E. (2022) The art of landslides: How stochastic mass wasting shapes topography and influences landscape dynamics. *Journal of Geophysical Research: Earth Surface*, 127(8), e2022JF006745. Available from: https://doi.org/10.1029/2022JF006745

Chatanantavet, P. & Parker, G. (2008) Experimental study of bedrock channel alluviation under varied sediment supply and hydraulic conditions. *Water Resources Research*, 44(12), W12446. Available from: https://doi.org/10.1029/2007WR006581

Chatanantavet, P. & Parker, G. (2009) Physically based modeling of bedrock incision by abrasion, plucking, and macroabrasion. *Journal of Geophysical Research*, 114(F4), F04018. Available from: https://doi.org/10.1029/2008JF001044

Croissant, T., Lague, D., Steer, P. & Davy, P. (2017) Rapid post-seismic landslide evacuation boosted by dynamic river width. *Nature Geoscience*, 10(9), 680–684. Available from: https://doi.org/10.1038/ngeo3005

Darling, A.L., Karlstrom, K.E., Granger, D.E., Aslan, A., Kirby, E., Ouimet, W.B. et al. (2012) New incision rates along the Colorado River system based on cosmogenic burial dating of terraces: Implications for regional controls on Quaternary incision. *Geosphere*, 8(5), 1020–1041. Available from: https://doi.org/10.1130/GES00724.1

Davy, P. & Lague, D. (2009) Fluvial erosion/transport equation of landscape evolution models revisited. *Journal of Geophysical Research*, 114(F3), F03007. Available from: https://doi.org/10.1029/2008JF001146

DeLisle, C., Yanites, B.J., Chen, C.-Y., Shyu, J. B.H. & Rittenour, T.M. (2022) Extreme event-driven sediment aggradation and erosional buffering along a tectonic gradient in southern Taiwan. *Geology*, 50(1), 16–20. Available from: https://doi.org/10.1130/G49304.1

Dingle, E.H., Attal, M. & Sinclair, H.D. (2017) Abrasion-set limits on Himalayan gravel flux. *Nature*, 544(7651), 471–474. Available from: https://doi.org/10.1038/nature22039

Dubinski, I.M. & Wohl, E. (2013) Relationships between block quarrying, bed shear stress, and stream power: A physical model of block quarrying of a jointed bedrock channel. *Geomorphology*, 180, 66–81. Available from: https://doi.org/10.1016/j.geomorph.2012.09.007

Duvall, A., Kirby, E. & Burbank, D. (2004) Tectonic and lithologic controls on bedrock channel profiles and processes in coastal California. *Journal of Geophysical Research*, 109(F3), F03002. Available from: https://doi.org/10.1029/2003JF000086

Ferguson, R.I. (2012) River channel slope, flow resistance, and gravel entrainment thresholds: Channel slope, flow resistance, and entrainment thresholds. *Water Resources Research* 48(5), 1–13. Available from: https://doi.org/10.1029/2011WR010850

Finnegan, N.J., Klier, R.A., Johnstone, S., Pfeiffer, A.M. & Johnson, K. (2017) Field evidence for the control of grain size and sediment supply on steady-state bedrock river channel slopes in a tectonically active setting. *Earth Surface Processes and Landforms*, 42(14), 2338–2349. Available from: https://doi.org/10.1002/esp.4187

Finnegan, N.J., Roe, G., Montgomery, D.R. & Hallet, B. (2005) Controls on the channel width of rivers: Implications for modeling fluvial incision of bedrock. *Geology*, 33(3), 229. Available from: https://doi.org/10.1130/G21171.1

Finnegan, N.J., Sklar, L.S. & Fuller, T.K. (2007) Interplay of sediment supply, river incision, and channel morphology revealed by the transient evolution of an experimental bedrock channel. *Journal of Geophysical Research: Earth Surface* 112(F3), 1–17. Available from: https://doi.org/10.1029/2006JF000569

Flint, J.J. (1974) Stream gradient as a function of order, magnitude, and discharge. *Water Resources Research*, 10(5), 969–973. Available from: https://doi.org/10.1029/WR010i005p00969

Foley, M.G. (1980) Bed-rock-incision by streams. *Geological Society of American Bulletin Part, II*, 91, 2189–2213.

Fuller, T.K. (2014) Field, experimental and numerical investigations into the mechanisms and drivers of lateral erosion in bedrock channels. Ph.D., University of Minnesota. Retrieved May 12, 2023, Available from: https://www.proquest.com/docview/1507869009/abstract/C6C2E151261F4BB3PQ/1

Gasparini, N.M., Bras, R.L. & Whipple, K.X. (2006) Numerical modeling of non-steady-state river profile evolution using a sediment-flux-dependent incision model. In: Willett, S. D., Hovius N., Brandon, M. T., Fisher, D. M. (Eds.) *Tectonics, climate, and landscape evolution*. Geological Society of America, pp. 127–141. Available from: https://doi.org/10.1130/2006.2398(08)

Gasparini, N.M., Tucker, G.E. & Bras, R.L. (1999) Downstream fining through selective particle sorting in an equilibrium drainage network. *Geology*, 27(12), 1079–1082.

Gasparini, N.M., Tucker, G.E. & Bras, R.L. (2004) Network–scale dynamics of grain–size sorting: Implications for downstream fining, stream–profile concavity, and drainage basin morphology. *Earth Surface Processes and Landforms*, 29(4), 401–421.

Gasparini, N.M., Whipple, K.X. & Bras, R.L. (2007) Predictions of steady state and transient landscape morphology using sediment-flux-dependent river incision models. *Journal of Geophysical Research*, 112(F3), F03S09. Available from: https://doi.org/10.1029/2006JF000567

Gilbert, G.K. (1877) *Report on the geology of the Henry Mountains*. US Government Printing Office: Washington.

Goode, J.R. & Wohl, E. (2010) Substrate controls on the longitudinal profile of bedrock channels: Implications for reach-scale roughness. *Journal of Geophysical Research: Earth Surface*, 115(F3), F03018. Available from: https://doi.org/10.1029/2008JF001188

Grant, G.E. (1997) Critical flow constrains flow hydraulics in mobile-bed streams: A new hypothesis. *Water Resources Research*, 33(2), 349–358. Available from: https://doi.org/10.1029/96WR03134

Hack, J.T. (1973) Stream-profile analysis and stream-gradient index. *Journal of Research of the us Geological Survey*, 1(4), 421–429.

Hergarten, S. (2020b) Transport-limited fluvial erosion - Simple formulation and efficient numerical treatment. *Earth Surface Dynamics*, 8, 841–854. Available from: https://doi.org/10.5194/esurf-8-841-2020

Hodge, R.A. & Hoey, T.B. (2016) A Froude-scaled model of a bedrock-alluvial channel reach: 2. Sediment cover. *Journal of Geophysical Research: Earth Surface*, 121(9), 1597–1618. Available from: https://doi.org/10.1002/2015JF003709

Hodge, R.A., Hoey, T.B. & Sklar, L.S. (2011) Bed load transport in bedrock rivers: The role of sediment cover in grain entrainment, translation, and deposition. *Journal of Geophysical Research: Earth Surface*, 116(F4), F04028. Available from: https://doi.org/10.1029/2011JF002032

Howard, A.D. (1994) A detachment-limited model of drainage basin evolution. *Water Resources Research*, 30(7), 2261–2285. Available from: https://doi.org/10.1029/94WR00757

Howard, A.D. & Kerby, G. (1983) Channel changes in badlands. *Geological Society of America Bulletin*, 94(6), 739. Available from: https://doi.org/10.1130/0016-7606(1983)94<CCIB>2.0.CO;2

Hurst, A.A., Anderson, R.S. & Crimaldi, J.P. (2021) Toward entrainment thresholds in fluvial plucking. *Journal of Geophysical Research: Earth Surface*, 126(5), e2020JF005944. Available from: https://doi.org/10.1029/2020JF005944

Inoue, T., Iwasaki, T., Parker, G., Shimizu, Y., Izumi, N., Stark, C.P. et al. (2016) Numerical simulation of effects of sediment supply on bedrock channel morphology. *Journal of Hydraulic Engineering*, 142(7), 4016014. Available from: https://doi.org/10.1061/(ASCE)HY.1943-7900.0001124

Johnson, J. P.L. (2014) A surface roughness model for predicting alluvial cover and bed load transport rate in bedrock channels. *Journal of Geophysical Research: Earth Surface*, 119(10), 2147–2173. Available from: https://doi.org/10.1002/2013JF003000

Johnson, J. P.L. & Whipple, K.X. (2010) Evaluating the controls of shear stress, sediment supply, alluvial cover, and channel morphology on experimental bedrock incision rate. *Journal of Geophysical Research: Earth Surface*, 115(F2), F02018. Available from: https://doi.org/10.1029/2009JF001335

Johnson, J. P.L., Whipple, K.X., Sklar, L.S. & Hanks, T.C. (2009) Transport slopes, sediment cover, and bedrock channel incision in the Henry

Mountains, Utah. *Journal of Geophysical Research: Earth Surface*, 114(F2), F02014. Available from: https://doi.org/10.1029/2007JF000862

Kodama, Y. (1994) Experimental study of abrasion and its role in producing downstream fining in gravel-bed rivers. *Journal of Sedimentary Research*, 64(1a), 76–85. Available from: https://doi.org/10.2110/jsr.64.76

Lague, D. (2014) The stream power river incision model: Evidence, theory and beyond. *Earth Surface Processes and Landforms*, 39(1), 38–61. Available from: https://doi.org/10.1002/esp.3462

Lai, L.S.-H., Roering, J.J., Finnegan, N.J., Dorsey, R.J. & Yen, J.-Y. (2021) Coarse sediment supply sets the slope of bedrock channels in rapidly uplifting terrain: Field and topographic evidence from eastern Taiwan. *Earth Surface Processes and Landforms*, 46(13), 2671–2689. Available from: https://doi.org/10.1002/esp.5200

Langston, A.L. & Temme, A. J. A.M. (2019) Impacts of lithologically controlled mechanisms on downstream bedrock valley widening. *Geophysical Research Letters*, 46(21), 12056–12064. Available from: https://doi.org/10.1029/2019GL085164

Langston, A.L. & Tucker, G.E. (2018) Developing and exploring a theory for the lateral erosion of bedrock channels for use in landscape evolution models. *Earth Surface Dynamics*, 6(1), 1–27. Available from: https://doi.org/10.5194/esurf-6-1-2018

Lavé, J. & Avouac, J.P. (2001) Fluvial incision and tectonic uplift across the Himalayas of central Nepal. *Journal of Geophysical Research: Solid Earth*, 106(B11), 26561–26591. Available from: https://doi.org/10.1029/2001JB000359

Leopold, L.B. & Maddock, T. (1953) *The hydraulic geometry of stream channels and some physiographic implications*, Vol. 252. US Government Printing Office.

Masteller, C.C., Finnegan, N.J., Turowski, J.M., Yager, E.M. & Rickenmann, D. (2019) History–dependent threshold for motion revealed by continuous bedload transport measurements in a steep mountain stream. *Geophysical Research Letters*, 46(5), 2583–2591. Available from: https://doi.org/10.1029/2018GL081325

Menting, F., Langston, A.L. & Temme, A. J. A.M. (2015) Downstream fining, selective transport, and hillslope influence on channel bed sediment in mountain streams, Colorado Front Range, USA. *Geomorphology*, 239, 91–105. Available from: https://doi.org/10.1016/j.geomorph.2015.03.018

Meshkova, L.V. & Carling, P.A. (2013) Discrimination of alluvial and mixed bedrock-alluvial multichannel river networks. *Earth Surface Processes and Landforms*, 38(11), 1299–1316. Available from: https://doi.org/10.1002/esp.3417

Meyer-Peter, E. & Müller, R. (1948) Formulas for bed-load transport, IAHSR 2nd Meeting, Stockholm. Appendix 2, pp. 39–64. Available from: https://repository.tudelft.nl/islandora/object/uuid%3A4fda9b61-be28-4703-ab06-43cdc2a21bd7

Mishra, J. & Inoue, T. (2020) Alluvial cover on bedrock channels: Applicability of existing models. *Earth Surface Dynamics*, 8(3), 695–716. Available from: https://doi.org/10.5194/esurf-8-695-2020

Montgomery, D.R. & Buffington, J.M. (1997) Channel-reach morphology in mountain drainage basins. *Geological Society of America Bulletin*, 109(5), 596–611. Available from: https://doi.org/10.1130/0016-7606(1997)109<0596:CRMIMD>2.3.CO;2

Montgomery, D.R. & Dietrich, W.E. (1992) Channel initiation and the problem of landscape scale. *Science*, 255(5046), 826–830. Available from: https://doi.org/10.1126/science.255.5046.826

Montgomery, D.R. & Foufoula-Georgiou, E. (1993) Channel network source representation using digital elevation models. *Water Resources Research*, 29(12), 3925–3934. Available from: https://doi.org/10.1029/93WR02463

Parker, G. (1978) Self-formed straight rivers with equilibrium banks and mobile bed. Part 2. The gravel river. *Journal of Fluid Mechanics*, 89(1), 127–146. Available from: https://doi.org/10.1017/S0022112078002505

Parker, G. (1991) Selective sorting and abrasion of river gravel. I: theory. *Journal of Hydraulic Engineering*, 117(2), 131–147. Available from: https://doi.org/10.1061/(ASCE)0733-9429(1991)117:2(131)

Parker, G., Wilcock, P.R., Paola, C., Dietrich, W.E. & Pitlick, J. (2007) Physical basis for quasi-universal relations describing bankfull hydraulic geometry of single-thread gravel bed rivers. *Journal of Geophysical Research*, 112(F4), F04005. Available from: https://doi.org/10.1029/2006JF000549

Pfeiffer, A.M., Finnegan, N.J. & Willenbring, J.K. (2017) Sediment supply controls equilibrium channel geometry in gravel rivers. *Proceedings of the National Academy of Sciences*, 114(13), 3346–3351. Available from: https://doi.org/10.1073/pnas.1612907114

Pfeiffer, A.M., Morey, S., Karlsson, H.M., Fordham, E.M. & Montgomery, D.R. (2022) Survival of the strong and dense: Field evidence for rapid, transport–dependent bed material abrasion of heterogeneous source lithology. *Journal of Geophysical Research: Earth Surface* 127(6). Available from: https://doi.org/10.1029/2021JF006455

Phillips, C.B. & Jerolmack, D.J. (2016) Self-organization of river channels as a critical filter on climate signals. *Science*, 352(6286), 694–697. Available from: https://doi.org/10.1126/science.aad3348

Phillips, C.B. & Jerolmack, D.J. (2019) Bankfull transport capacity and the threshold of motion in coarse–grained rivers. *Water Resources Research*, 55(12), 11316–11330. Available from: https://doi.org/10.1029/2019WR025455

Phillips, C.B., Masteller, C.C., Slater, L.J., Dunne, K. B.J., Francalanci, S., Lanzoni, S. et al. (2022) Threshold constraints on the size, shape and stability of alluvial rivers. *Nature Reviews Earth and Environment*, 3(6), 406–419. Available from: https://doi.org/10.1038/s43017-022-00282-z

Pitlick, J. & Cress, R. (2002) Downstream changes in the channel geometry of a large gravel bed river: Downstream changes in channel geometry. *Water Resources Research*, 38(10), 34–1–34-11. Available from: https://doi.org/10.1029/2001WR000898

Rickenmann, D. (2001) Comparison of bed load transport in torrents and gravel bed streams. *Water Resources Research*, 37(12), 3295–3305. Available from: https://doi.org/10.1029/2001WR000319

Rickenmann, D. & Recking, A. (2011) Evaluation of flow resistance in gravel-bed rivers through a large field data set: Evaluation of flow resistance equations. *Water Resources Research*, 47(7), W07538. Available from: https://doi.org/10.1029/2010WR009793

Seidl, M. & Dietrich, W.E. (1992) The problem of channel erosion into bedrock. CATENA SUPPLEMENT.

Shields, A. (1936) Anwendung Der Aehnlichkeitsmechanik Und Der Turbulenzforschung Auf Die Geschiebebewegung. Doktor-ingenieurs dissertation, Technische Hochschule Berlin.

Shobe, C.M., Tucker, G.E. & Anderson, R.S. (2016) Hillslope–derived blocks retard river incision. *Geophysical Research Letters*, 43(10), 5070–5078. Available from: https://doi.org/10.1002/2016GL069262

Shobe, C.M., Tucker, G.E. & Barnhart, K.R. (2017) The SPACE 1.0 model: A Landlab component for 2-D calculation of sediment transport, bedrock erosion, and landscape evolution. *Geoscientific Model Development*, 10(12), 4577–4604. Available from: https://doi.org/10.5194/gmd-10-4577-2017

Sklar, L. & Dietrich, W.E. (1998) River longitudinal profiles and bedrock incision models: Stream power and the influence of sediment supply. *Geophysical Monograph-American Geophysical Union*, 107, 237–260.

Sklar, L.S. & Dietrich, W.E. (2001) Sediment and rock strength controls on river incision into bedrock. *Geology*, 29(12), 1087. Available from: https://doi.org/10.1130/0091-7613(2001)029<1087:SARSCO>2.0.CO;2

Sklar, L.S. & Dietrich, W.E. (2004) A mechanistic model for river incision into bedrock by saltating bed load: Bedrock incision by saltating bed load. *Water Resources Research*, 40(6), W06301. Available from: https://doi.org/10.1029/2003WR002496

Sklar, L.S., Dietrich, W.E., Foufoula-Georgiou, E., Lashermes, B. & Bellugi, D. (2006) Do gravel bed river size distributions record channel network structure? *Water Resources Research*, 42(6), W06D18. Available from: https://doi.org/10.1029/2006WR005035

Sklar, L.S., Riebe, C.S., Marshall, J.A., Genetti, J., Leclere, S., Lukens, C.L. et al. (2017) The problem of predicting the size distribution of sediment supplied by hillslopes to rivers. *Geomorphology*, 277, 31–49.

Tarboton, D.G., Bras, R.L. & Rodriguez-Iturbe, I. (1989) Scaling and elevation in river networks. *Water Resources Research*, 25(9), 2037–2051. Available from: https://doi.org/10.1029/WR025i009p02037

Tofelde, S., Bufe, A. & Turowski, J.M. (2022) Hillslope sediment supply limits alluvial valley width. *AGU Advances*, 3(6), e2021AV000641. Available from: https://doi.org/10.1029/2021AV000641

Tucker, G.E. & Whipple, K.X. (2002) Topographic outcomes predicted by stream erosion models: Sensitivity analysis and intermodel comparison. *Journal of Geophysical Research: Solid Earth*, 107(B9), 2179. Available from: https://doi.org/10.1029/2001JB000162

Turowski, J.M. & Hodge, R. (2017) A probabilistic framework for the cover effect in bedrock erosion. *Earth Surface Dynamics*, 5(2), 311–330.

Turowski, J.M., Lague, D. & Hovius, N. (2007) Cover effect in bedrock abrasion: A new derivation and its implications for the modeling of bedrock channel morphology. *Journal of Geophysical Research: Earth Surface*, 112(F4), F04006. Available from: https://doi.org/10.1029/2006JF000697

Whipple, K.X. (2004) Bedrock rivers and the geomorphology of active orogens. *Annual Review of Earth and Planetary Sciences*, 32(1), 151–185. Available from: https://doi.org/10.1146/annurev.earth.32.101802.120356

Whipple, K.X., Hancock, G.S. & Anderson, R.S. (2000) River incision into bedrock: Mechanics and relative efficacy of plucking, abrasion, and cavitation. *Geological Society of America Bulletin*, 112(3), 490–503. Available from: https://doi.org/10.1130/0016-7606(2000)112<490:RIIBMA>2.0.CO;2

Whipple, K.X. & Tucker, G.E. (1999) Dynamics of the stream-power river incision model: Implications for height limits of mountain ranges, landscape response timescales, and research needs. *Journal of Geophysical Research: Solid Earth*, 104(B8), 17661–17674. Available from: https://doi.org/10.1029/1999JB900120

Whipple, K.X. & Tucker, G.E. (2002) Implications of sediment-flux-dependent river incision models for landscape evolution. *Journal of Geophysical Research: Solid Earth*, 107(B2), ETG 3–1-ETG 3–20. Available from: https://doi.org/10.1029/2000JB000044

Whittaker, A.C., Cowie, P.A., Attal, M., Tucker, G.E. & Roberts, G.P. (2007) Bedrock channel adjustment to tectonic forcing: Implications for predicting river incision rates. *Geology*, 35(2), 103. Available from: https://doi.org/10.1130/G23106A.1

Wickert, A.D. & Schildgen, T.F. (2019) Long-profile evolution of transport-limited gravel-bed rivers. *Earth Surface Dynamics*, 7(1), 17–43. Available from: https://doi.org/10.5194/esurf-7-17-2019

Wilcock, P.R., Kenworthy, S.T. & Crowe, J.C. (2001) Experimental study of the transport of mixed sand and gravel. *Water Resources Research*, 37(12), 3349–3358. Available from: https://doi.org/10.1029/2001WR000683

Willgoose, G., Bras, R.L. & Rodriguez-Iturbe, I. (1991a) A coupled channel network growth and hillslope evolution model: 1. *Theory*. *Water Resources Research*, 27(7), 1671–1684. Available from: https://doi.org/10.1029/91WR00935

Willgoose, G., Bras, R.L. & Rodriguez-Iturbe, I. (1991b) A coupled channel network growth and hillslope evolution model: 2. Nondimensionalization and applications. *Water Resources Research*, 27(7), 1685–1696. Available from: https://doi.org/10.1029/91WR00936

Willgoose, G., Bras, R.L. & Rodriguez-Iturbe, I. (1991c) A physical explanation of an observed link area-slope relationship. *Water Resources Research*, 27(7), 1697–1702. Available from: https://doi.org/10.1029/91WR00937

Wong, M. & Parker, G. (2006) Reanalysis and correction of bed-load relation of Meyer-Peter and Müller using their own database. *Journal of Hydraulic Engineering*, 132(11), 1159–1168. Available from: https://doi.org/10.1061/(ASCE)0733-9429(2006)132:11(1159)

Yanites, B.J., Mitchell, N.A., Bregy, J.C., Carlson, G.A., Cataldo, K., Holahan, M. et al. (2018) Landslides control the spatial and temporal variation of channel width in southern Taiwan: Implications for landscape evolution and cascading hazards in steep, tectonically active landscapes. *Earth Surface Processes and Landforms*, 43(9), 1782–1797. Available from: https://doi.org/10.1002/esp.4353

Yanites, B.J., Tucker, G.E., Hsu, H.-L., Chen, C., Chen, Y.-G. & Mueller, K.J. (2011) The influence of sediment cover variability on long-term river incision rates: An example from the Peikang River, central Taiwan. *Journal of Geophysical Research: Earth Surface*, 116(F3), F03016. Available from: https://doi.org/10.1029/2010JF001933

Yanites, B.J., Tucker, G.E., Mueller, K.J., Chen, Y.-G., Wilcox, T., Huang, S.-Y. et al. (2010) Incision and channel morphology across active structures along the Peikang River, central Taiwan: Implications for the importance of channel width. *Geological Society of America Bulletin*, 122(7-8), 1192–1208. Available from: https://doi.org/10.1130/B30035.1

Zhang, L., Parker, G., Stark, C.P., Inoue, T., Viparelli, E., Fu, X. & Izumi, N. (2015) Macro-roughness model of bedrock-alluvial river morphodynamics. *Earth Surface Dynamics*, 3(1), 113–138. Available from: https://doi.org/10.5194/esurf-3-113-2015

SUPPORTING INFORMATION

Additional supporting information can be found online in the Supporting Information section at the end of this article.

How to cite this article: Gabel, V., Tucker, G.E. & Campforts, B. (2024) A mathematical model for bedrock incision in near-threshold gravel-bed rivers. *Earth Surface Processes and Landforms*, 49(13), 4168–4186. Available from: https://doi.org/10.1002/esp.5957